



Contents lists available at ScienceDirect

Proceedings of the Geologists' Association

journal homepage: www.elsevier.com/locate/pgeola

A reassessment of Arundian–Holkerian (Viséan) carbonates in South Cumbria, UK

Mark W. Hounslow^{a,b,*}, Ian D. Somerville^c, Pedro Cózar^d, David Chew^e, Foteini Drakou^e

^a Lancaster Environment Centre, Lancaster University, Lancaster LA1 4YW, UK

^b Earth, Ocean and Ecological Sciences, University of Liverpool, Jane Herdman Building, Liverpool L69 3GP, UK

^c UCD School of Earth Sciences, University College Dublin, Ireland

^d Instituto de Geociencias (CSIC-UCM), c/ Severo Ochoa 7, 28040 Madrid, Spain

^e Department of Geology, Trinity College Dublin, Ireland

ARTICLE INFO

Article history:

Received 17 December 2021

Received in revised form 9 April 2022

Accepted 21 April 2022

Available online xxxxx

Keywords:

Viséan

Foraminiferal biostratigraphy

Lithostratigraphy

Microfacies

Dalton Formation

Red Hill Limestone Formation

ABSTRACT

Despite the importance of south Cumbrian sections for the Arundian–Holkerian (mid Viséan) boundary, beyond the stratotype proposed at Barker Scar in 1976, little else is known regionally about this boundary and its relationship to adjacent formations. We re-evaluate the Dalton Formation, making its upper and lower boundaries regionally more consistent and precisely-defined, in good quality outcrops with associated biostratigraphy. The Dalton Formation is formally divided into the Blackstone Member and overlying Raven's Member. Rich foraminiferal assemblages of the Cf4 δ subzone are recognised in the Blackstone Member and the lower to mid Raven's Member in nine sections. The Cf4 γ –Cf4 δ boundary is recognised in the underlying Red Hill Limestone Formation in 3 sections. The upper part of the Raven's Member shows the first appearance of taxa assigned to the Cf5 α and Cf5 β subzones of the Holkerian in three of the sections. Bentonitic shales in the mid and upper-most part of the Raven's Member were evaluated for zircon and apatite geochronology, although only 4 out of 504 analyses yielded Carboniferous ages, indicating an almost entirely detrital source. This detritus was northerly or northeasterly-derived and predominantly from the Southern Uplands Terrane with subsidiary input from the Lewisian Complex or eastern Greenland sources. Petrographic analysis identified 13 microfacies indicating that the Dalton Formation represents the inner to outer part of a southward inclined shelf, in which east–west changes in microfacies were generated by synsedimentary faulting inherited from northwest–southeast aligned basement structures.

© 2022 The Geologists' Association. Published by Elsevier Ltd. This is an open access article under the CC BY license (<http://creativecommons.org/licenses/by/4.0/>).

1. Introduction

From studies covering the Furness to Arnside–Carnforth to Kendal regions (south Cumbria and north Lancashire), the importance of this region for the British Lower Carboniferous stratigraphy was first established by the pioneering studies of Garwood (1913, 1916). This author revised the biostratigraphic zones of Vaughan (1905) and proposed the main biostratigraphic markers and faunal assemblage subzones and 'bands' in NW England, which have been widely utilised by subsequent authors (Fig. 1). The index macrofossils of Garwood's subzones have also been widely used in the lithostratigraphic studies in northern England over many decades within the Great Scar Limestone Group (Dean et al., 2011, 2021), although, as noted by Rose and Dunham (1977), the range of the eponymous fauna of Garwood's bands and

assemblage subzones extended beyond his sub-divisions—as also admitted by Garwood.

The significance of the lithostratigraphic divisions in south Cumbria was emphasised by the selection of the (chronostratigraphic) basal Holkerian stratotype by George et al. (1976) at Barker Scar, near Holker Hall (Fig. 2). They selected the boundary stratotype at the junction of the 'Dalton Beds' and the 'Park Limestone' of Dunham and Rose (1941) and Rose and Dunham (1977). Later, these units were formally designated as the Dalton and Park Limestone formations (Johnson et al., 2001) (Fig. 1). Undoubtedly, the joining of lithostratigraphic and British chronostratigraphic stages at a single level in the rock record for the base Holkerian was strongly impacted by the influential work of Ramsbottom (1973), which in essence linked these types of stratigraphy to inferred eustatic control. As noted by Riley (1993) this useful and ground-breaking approach was a rather unwise binding of stratigraphic concepts, rather loosely linked to biostratigraphy. The lithological expression of the basal Holkerian boundary in successions in south Cumbria was also poorly defined, opening it up to later criticism (Johnson et al., 2001; Waters et al., 2009, 2021). Here we separate the basal

* Corresponding author at: Lancaster Environment Centre, Lancaster University, Lancaster LA1 4YW, UK.

E-mail address: mark.w.hounslow@gmail.com (M.W. Hounslow).

<https://doi.org/10.1016/j.pgeola.2022.04.005>

0016-7878/© 2022 The Geologists' Association. Published by Elsevier Ltd. This is an open access article under the CC BY license (<http://creativecommons.org/licenses/by/4.0/>).

Substage		Vaughan (1905)		Garwood (1913)		Key coral taxa	Johnson et al. (2001)	Thomas (2009)	Millward et al. (2010)	This study	
		Zones	Subzones	Zones	Subzones					Lithostratigraphy	Foraminiferal zones
Brigantian (part)	early	Lonsdaleia (D2)	Dibunophyllum (D)	Dibunophyllum (D)	Lonsdaleia floriformis (D2)	Actinocyathus floriformis Palastraea regia	Gleaston Formation	Alston Formation	Cf6δ	Brigantian (part)	
	late				θφ (D1)	Cyathophyllum murchisoni (D1)					Dibunophyllum bipartitum Lithostroton maccoyanum Siphonodendron junceum
Asbian	early				Lithostroton decipiens Siphodendron pauciradiale						
	late				Nematophyllum minus Cyrtina carbonaria (S2)	Diphyphyllum smithi Lithostroton araneum Lithostroton vorticale Siphodendron scaleberense	Park Limestone Formation	Park Limestone Formation	Park Limestone Formation	Cf6α-β Cf5β2 Cf5β1	Holkerian
Holkerian	early				Gastropod Beds (S1 part)	Dorlodotia briarti Siphonodendron sociale					
	late	S2 (part)	Seminula (S)	Productus corrugatohemisphaericus (S)	Chonetes carinata (C2) Camarophoria isorhyncha (C2)	Clisiophyllum multiseptatum	Dalton Formation	Dalton Formation	Dalton Fm	Raven's Member Blackstone Member	Cf5α Cf4δ upper middle lower Cf4γ
Arundian (part)	mid	Syringothyris (C) part		Michelina grandis			Red Hill Limestone Fm	Red Hill Limestone Formation	Red Hill Limestone Formation		
	late	S1									

Fig. 1. Comparison of the coral biozonation schemes of Vaughan (1905) for the Bristol area, Garwood (1913) for northern England, updated key rugose corals and brachiopods, and lithostratigraphy of the region in Johnson et al. (2001), and in this study (using Cózar et al., 2022, in press). Adapted from Waters et al. (2021). Abbreviations: m middle, W Woodbine Shale, HH Humphreys Head Limestone Member, HL Hawes Limestone, KC Kettlewell Crag Member. Dark grey intervals are inferred missing. The columns of Johnson et al. (2001), Thomas (2009) and Millward et al. (2010) relate to the Furness–Carmel peninsulas, Yewbarrow and Kendal blocks, respectively (Fig. 2).

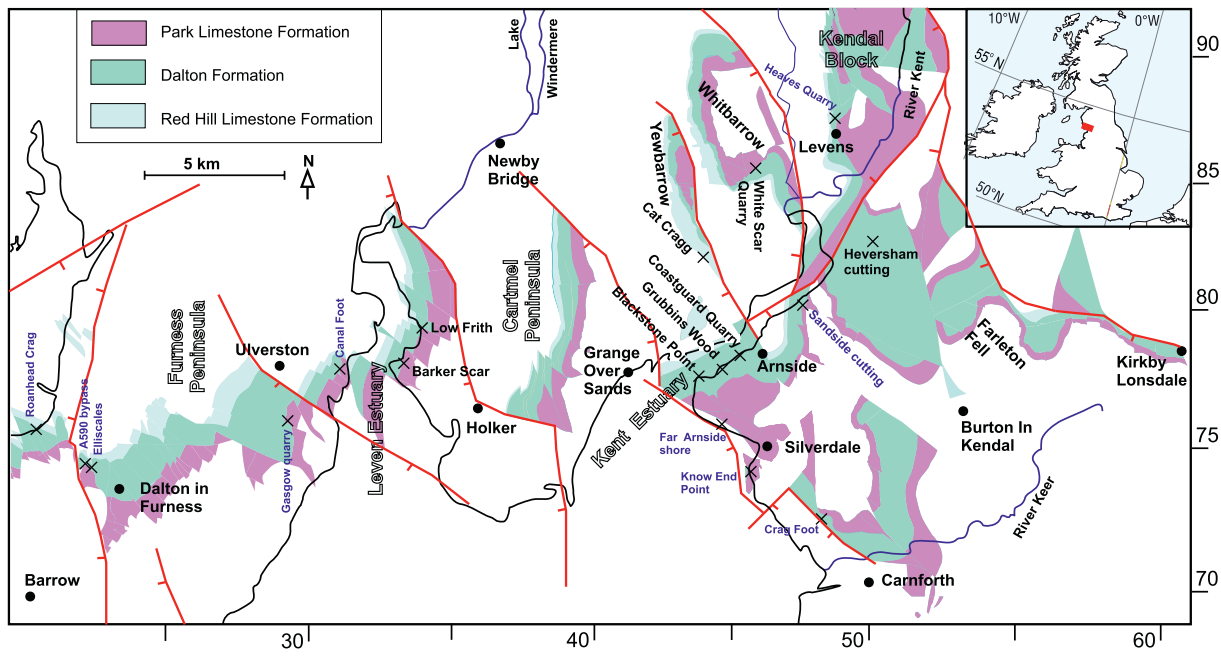


Fig. 2. Map of the studied stratigraphic sections in south Cumbria and north Lancashire, overlain on the distribution of the Arundian (Red Hill Limestone Fm, Dalton Fm) and Holkerian (Park Limestone Fm) units. Map based on Digimap data. Crosses = sections, dots = towns and villages. Additional sections (in blue) not detailed here, but mentioned in text are listed in SI Table S1. Inset shows location in Britain. Major faults with downthrow direction shown in red; rivers/lakes in blue. Border numbers are British Ordnance Survey grid references. (For interpretation of the references to colour in this figure legend, the reader is referred to the web version of this article.)

Holkerian chronostratigraphy and lithostratigraphy and instead bind it more precisely to the biostratigraphy.

1.1. The nature of former divisions in the Dalton Formation

The Viséan outcrops in the region of south Cumbria and north Lancashire are broken into a series of eastward-tilted fault blocks north of the River Kent and Kent Estuary and southeast-tilted blocks southeast of the Kent Estuary and in Furness (Fig. 2). This faulting has segmented the continuity of the outcropping successions into a series of distinct blocks and regions, which have somewhat differing successions (Figs. 1, 2).

The basis for the lithostratigraphic subdivision used by Rose and Dunham (1977) and Johnson et al. (2001) was centred on data from mine workings, drillcore and outcrop sections from west of Grange-over-Sands (Fig. 2). In fact, now, with the demise of mining in the Furness Peninsula, many of the more-complete, less mineralised, less karstified and less dolomitised, mid-Viséan sections lie east of the Cartmel Peninsula, but have been little studied since Garwood's work.

Rose and Dunham (1977) described the Dalton Beds as a dark grey, medium-grained limestone, bituminous and foetid; typically separated by thin shales along well-marked undulating bedding planes. A marked shaley interval present in the Dalton Beds is most distinctive and acted as a middle division of the three parts to the Dalton Beds. The limestones in the upper part of the formation can be sandy and/or dolomitic in some stratigraphic sections, whereas the lower and middle part is characterised by the brachiopod "*Chonetes*" (= *Delepineia*) *carinata* (Rose and Dunham, 1977). The Park Limestone, in contrast to the limestones of the Dalton Beds, is a cream to pale grey limestone marked by a lack of argillaceous material and often indistinct bedding.

Following Rose and Dunham (1977), Johnson et al. (2001) also used a tripartite subdivision of the Dalton Formation, considering the three lithostratigraphical units as informal members, named as lower, middle and upper. However, the characterisation of the lower unit differs in the two accounts, and Rose and Dunham (1977) offered no type section of the Dalton Beds, although strata exposed in the cliffs of the east coast of the Leven Estuary (around Barker Scar, Fig. 2) provided their longest and most detailed lithologic logs. Johnson et al. (2001) suggested a type section of the Dalton Formation in the A590 Dalton-in-Furness bypass (A590-bypass in Fig. 2), although, this section is heavily faulted and now largely overgrown with vegetation. Most of the adjacent quarry at Elliscales and its *Syringopora*-*Aphralysia*-algal reefs (Nicholas, 1968; Adams, 1984) were considered part of the lower division by Johnson et al. (2001), although lithologically, the dolomitised off-reef beds are most like the Red Hill Limestone Formation (Nicholas, 1968; Adams, 1984). Rose and Dunham (1977, p. 46) assigned the lower boundary of the Dalton Beds at 6 m below the top of the Elliscales Quarry section. The lower member of the Dalton Formation of Johnson et al. (2001) and Rose and Dunham (1977) was also associated with outcrops at Low Frith (Leven Estuary, Fig. 2) of Red Hill Limestone-type lithology bearing "*Chonetes*" (*Delepineia*) *carinata* (Garwood, 1916). In contrast, the mapping work of Thomas (2009) in the Yewbarrow area (Figs. 1, 2) placed the base of the Dalton Formation at the base of the middle shaley division. Further south on the Arnside shore, a shale-rich interval in the Dalton Formation rests on pale peloidal grainstones, here assigned to the Red Hill Limestone Formation, like in the Yewbarrow area (Figs. 1, 2).

The relationship between faunal subzones and bands of Garwood (1913) and the modern lithostratigraphy can be best estimated from Garwood's maps and descriptions of coastal sections along the Leven Estuary and at Arnside. The "*Chonetes*" (= *Delepineia*) *carinata* Subzone includes largely, the upper part of the Red Hill Limestone Formation (as used here), and most of the middle division of the Dalton Formation (Fig. 1). In contrast, in the Yewbarrow area the base of the "*Ch.*" *carinata* Subzone is near the base of the Red Hill Limestone Formation (compare maps in Garwood, 1913 and Thomas, 2009). At Elliscales, Garwood (1913, p. 533) placed the base of the "*Ch.*" *carinata* Subzone above the Elliscales quarry section (which was placed in the underlying

Camarophoria isorhyncha Subzone). Hence, at Elliscales, the base of the Dalton Formation (as used by Rose and Dunham (1977) and Johnson et al., 2001) is within the *Camarophoria isorhyncha* Subzone (Fig. 1). Garwood's *Clisiophyllum multiseptatum* Band (a solitary coral-bearing shaley band) is developed near the top of the shaley middle division (well exposed at Barker Scar, Blackstone Point and Low Frith). The Gastropod Beds (Fig. 1) of Garwood (1913) relate to most of the upper lithostratigraphic division of the Dalton Formation and the lower part of the Park Limestone (best developed in the Arnside area and Barker Scar; SI Fig. S1). Rather inconsistently, Johnson et al. (2001, p. 59) suggested the "*Ch.*" *carinata* Subzone, *C. multiseptatum* Band and the Gastropod Beds of Garwood constitute "approximately" the three informal members of the Dalton Formation (Fig. 1). Undoubtedly the base of Garwood's "*Ch.*" *carinata* Subzone acted as a suitable base-of-formation guide in some other parts of S. Cumbria. Hence, perhaps out of graphical convenience (or the imprecision of Garwood's subzones in the lithostratigraphic succession), both Rose and Dunham (1977) and Johnson et al. (2001) made Garwood's subzonal boundaries and the lithostratigraphic boundaries erroneously coincident (Fig. 1).

Garwood's overlying '*Cyrtina* (= *Davidsonina*) *carbonaria*' Subzone cannot be distinguished in most of south Cumbria, other than near Kendal (Garwood, 1913) and the '*Nematophyllum minus*' (= *Lithostrotion araneum* McCoy, 1844) Subzone covers the remainder of the Park Limestone Formation (Fig. 1).

1.2. Defining the Arundian–Holkerian boundary

At the Barker Scar 'reference' section, the base of the Holkerian was positioned at the base of bed k following the bed nomenclature of Rose and Dunham (1977), who first described the section (beds were later relabelled in capital letters by Ramsbottom, 1981). Although it is claimed that there is a marked colour change here between the Dalton Formation and Park Limestone Formation (dark grey to paler grey), this is strongly conditioned by the locally dolomitic and grainstone-bearing nature of the upper part of the Dalton Formation. A much better distinction is the lack of argillaceous beds in the Park Limestone Formation. Johnson et al. (2001) selected bed J as the base of the Park Limestone Formation due to the start of poorly developed bedding and close jointing, features more typical of the Park Limestone. In contrast, Balderstone and Dewey (2003) working in the Arnside–Silverdale area on this boundary (at the Far Arnside and Know End Point sections; Fig. 2), placed the base of the Holkerian in the uppermost part of their 'Dalton formation', utilising the lowest occurrence of *L. araneum*, with the base of the Park Limestone Formation, at the top of a prominent coral-bearing limestone bed several metres higher in the sections. The placement used by Balderstone and Dewey (2003) is erroneous, since limestones in the Know End Point section are of early Asbian age (our unpublished data) and belong to the mid parts of the Park Limestone Formation. In spite of these divergences of view, at Barker Scar the base of the Park Limestone Formation has commonly been placed at the base of bed J, and the base of the Holkerian commonly placed at the base of bed K (see e.g., Cossey et al., 2004; Waters et al., 2011; Dean et al., 2011).

However, the foraminiferal-defined base of the Holkerian in the Barker Scar section has now been revised (Cózar et al., 2022), demonstrating that the microfauna previously proposed by George et al. (1976), Conil et al. (1980), Ramsbottom (1981), Strank (1981) and Fewtrell et al. (1981), as well as other worldwide middle Viséan taxa (Cózar et al., 2020a), first occur in much lower levels in the Barker Scar section, at bed C. Cózar et al. (2022), proposed to reposition the base of the Holkerian to coincide with the foraminiferal markers at bed C in the upper Dalton Formation, thereby, giving the base Holkerian a robust international correlation with the middle Viséan. The alternative position of maintaining the base of the Holkerian at bed K is problematic, since there are no fossil markers to recognise it beyond Barker Scar. The dolomitic character of the upper part of the Dalton Formation in the Barker Scar section, as well as the presence of common sandy

Table 1
Sections studied in detail in the Dalton Formation and those crossing its lower and upper boundaries.

Section	Location [SD grid ref., latitude/longitude (°, ', ")	Formations (members) exposed [n].	Subzonal position of Garwood (1913)
Low Frith	Levens Estuary [339796], N54,12,27; W3,0,46	um Red Hill Limestone to Dalton Limestone (lp Raven's) [30]	<i>D. carinata</i>
Barker Scar	Levens Estuary [333783], N54,11,50/W3,1,28	Dalton Limestone (up. Blackstone, Raven's), lp Park Limestone	<i>D. carinata</i> to Gastropod Beds
White Scar Quarry	Whitbarrow [458850], N54,15,27/W2,50,04	Dalton Limestone (Blackstone, Raven's), most of Park Limestone [47]	<i>N. minus?</i>
Heversham cutting Coastguard Quarry ^a	Milnthorpe [499830], N54,14,23; W2,46,03 Arnside [452784], N54,11,54/W2,50,35	Dalton Limestone (Blackstone, lp Raven's) [2] um Red Hill Limestone to Dalton Limestone (Blackstone, Raven's) [24]	Gastropod Beds <i>D. carinata</i>
Grubbins Wood ^b	Arnside [445779], N54,11,37/W2,51,12	um Red Hill Limestone, Dalton Limestone (Blackstone, Raven's) to base Park Limestone [75]	<i>D. carinata</i> –Gastropod Beds
Blackstone Point	Arnside [436776] N54,11,27; W2,51,42	um Red Hill Limestone to Dalton Limestone (Blackstone, lp–mp Raven's) [31]	<i>D. carinata</i> –Gastropod Beds
Cat Cragg Quarry	Yewbarrow [438824], N54,14,4; W2,51,51	lp Red Hill Limestone Formation [13]	<i>C. isorhyncha</i> –basal <i>D. carinata</i>

Up = upper part, lp = lower part, mp = mid part, um = uppermost. [n] = number of sampled studied herein.

^a 'Mr Crossfield's boat-house to corporation bathing shed description' of Garwood (1913).

^b Grubbins Wood sub sections are from the bases 2a, 2b and 1. See Supplementary information for details.

beds (notably barren in foraminifers), does not allow recognition of continuous phylogenetic lineages, nor does it ensure that the first occurrence of the key taxa might not be different in better preserved, less dolomitised sections.

The aims for this study are: (i) to revise the lithostratigraphy of the Dalton Formation for S. Cumbria and N. Lancashire in order to propose more regionally-recognisable formation boundaries; (ii) to propose a revised lithostratigraphic division of the Dalton Formation, including new more regionally-robust formal members within the formation; (iii) to examine the potential of U–Pb zircon–apatite geochronology in newly discovered bentonitic beds in the Dalton Formation; (iv) to revise the foraminifers of this interval to corroborate the biostratigraphical zones and subzones; and (v) to provide a detailed petrographic microfacies analysis of sections leading to a refined regional facies model of the Dalton Formation.

2. Studied sections and material

The study sections are detailed in Table 1 and locations shown in Figure 2. More detailed sketch maps of the key sections are shown in Supplementary (SI) Figures S1 to S3.

In total, 336 levels/horizons have been sampled in the ten logged sections and the number of thin-sections prepared for the analysis of the microfacies and foraminifers amounts to 785 standard thin-sections (28 × 48 mm) which are housed in the Palaeontology area of the University Complutense Madrid. Details of the samples from the Barker Scar section were published in Cózar et al. (2022). Classifications by Dunham (1962) and Embry and Klovan (1971) were used to describe the microfacies. The abundance of grains, cement and matrix were visually estimated using the charts of Baccelle and Bosellini (1965) and are detailed in the Supplementary data. The sedimentary logs were constructed from additional field observations, and an additional sample set not shown here, and for these reasons the logs are more detailed than the apparent sampling points used for thin sections.

Zircon and apatite U–Pb LA-ICP-MS dating on bentonitic layers within the upper Part of the Dalton Fm at White Scar Quarry (Fig. 3) was undertaken at Trinity College Dublin, Ireland, to determine if these had potential for high-precision U–Pb zircon geochronology (e.g., isotope dilution–thermal ionisation mass spectrometry). The geochronology analytical technique and isotopic data are provided in the Supplementary material.

3. Field and member descriptions of the Dalton Formation

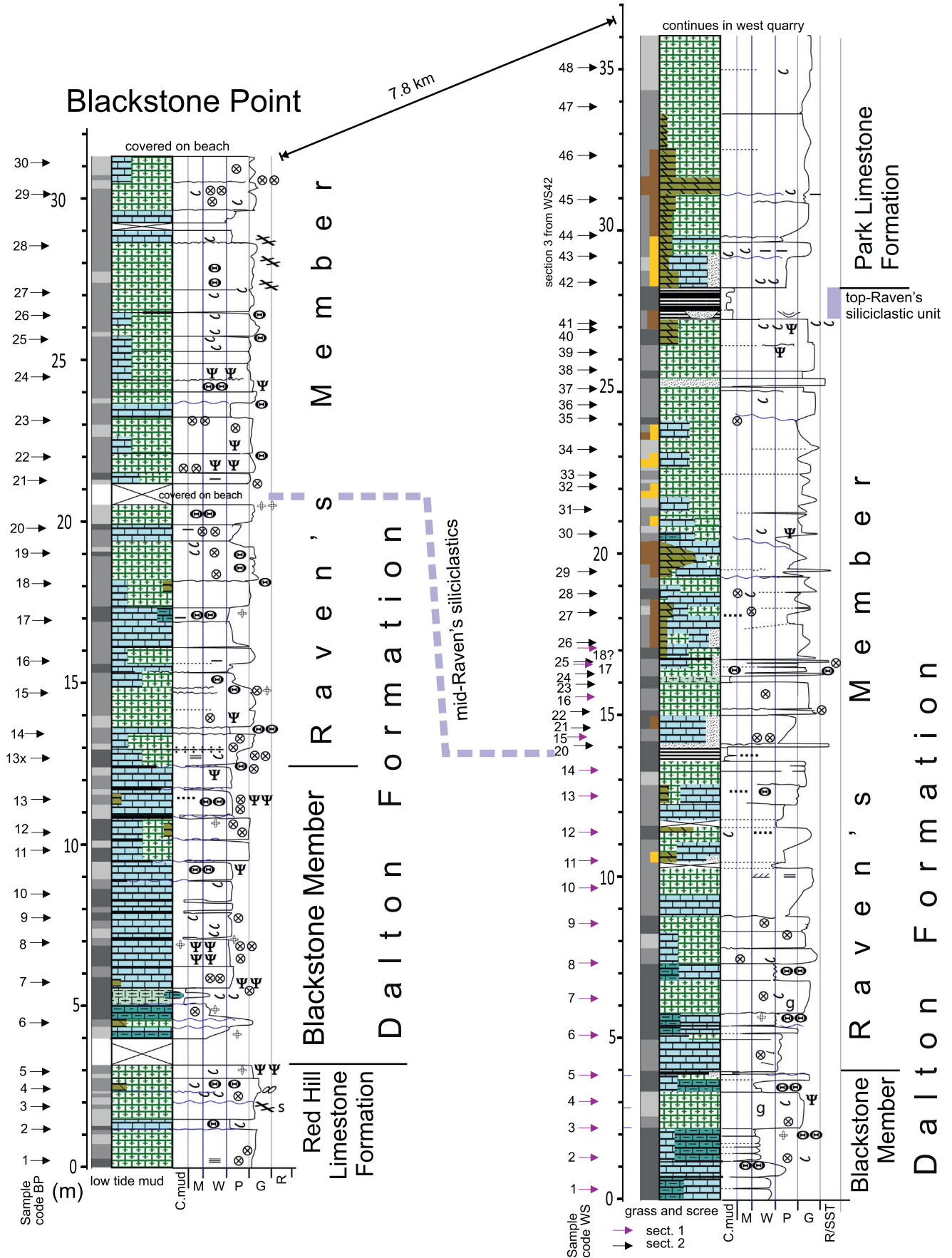
Two new formal members are proposed for the Dalton Formation: a lower Blackstone Member, with a type section at Blackstone Point (Figs. 2, 3 and SI Fig. S1). This is succeeded by the Raven's Member for the upper part of the Dalton Formation, with a type section at White Scar Quarry near Raven's Lodge Farm, between Levens and Yewbarrow (Figs. 2, 3, SI Fig. S3). The combined thickness of both members ranges from ca. 31 m in the Leven Estuary area, to 50.5 m on the Arnside shore, reaching a maximum thickness of ca. 64 m at Farleton Fell (Figs. 1, 2, SI Fig. S4). Existing sections in the Furness Peninsula do not allow thicknesses to be estimated using definitions as used here.

3.1. Blackstone Member

The Blackstone Member is 7–16 m thick: The base of the member can be located at Blackstone Point (type section; Fig. 3) and Coastguard Quarry, where the basal shaley interval rests probably conformably, on typically thicker-bedded, pale grey peloidal grainstones (interpreted as the underlying Red Hill Limestone Formation; Figs. 3, 4). The Blackstone Member is composed of beds of typically dark grey wackestone to wackestone–packstone interbedded with shale, mudstone and calcareous mudstone (Figs. 3, 5). The upper part of the member may contain grainstones in some sections. On the Arnside shore both the base of the Blackstone Member and the top-most Red Hill Limestone Formation are intermittently exposed (due to minor faulting and gentle folding) on the shore northeastwards from Blackstone Point to Grubbins Wood to Coastguard Quarry to Ash Meadow House at Arnside (see Figs. 2, 4–6; SI Fig. S1). The thickness and frequency of shale–mudstone beds decrease upwards in the succession and where these argillaceous interbeds are reduced to less than 5% of the interval, this point is taken as the top of the member. The member corresponds approximately with the middle division of Rose and Dunham (1977) and Johnson et al. (2001), and the lower part of the Dalton Formation of Thomas (2009). The unit corresponds to the upper part of the 'Chonetes' *carinata* Subzone of Garwood (1913) along the shoreline west of Arnside, and in the Leven Estuary at Low Frith (Figs. 1, 7, SI Fig. S6). In the Furness area, presently the best representation of the basal Dalton Formation is at Roanhead Crag where it overlies some 45 m of the Red Hill Limestone Formation (Nicholas, 1968; Rose and Dunham, 1977; Fig. 2). The Blackstone Member is a common source of springs, so can be approximately located in areas with no exposure during

Fig. 3. Stratigraphic sections at Blackstone Point and White Scar Quarry (eastern side), the type sections of the Blackstone and Raven's members respectively (see Fig. 2 for location and Fig. 7 for the key). Arrows show section sample numbers and positions. C.mud = clastic mudstone/shale, M, W, P, G, R/SST = mudstone, wackestone, packstone, grainstone, rudstone/sandstone respectively. Distance between sections shown.

E. White Scar Quarry



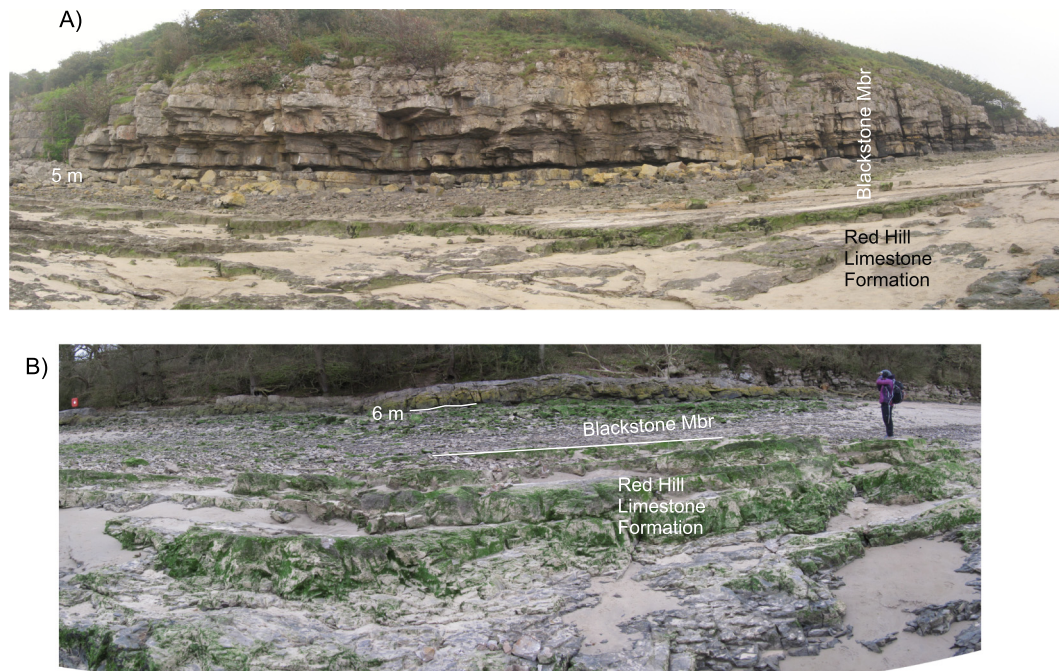


Fig. 4. The Red Hill Limestone Formation–Dalton Formation (Blackstone Member) boundary at: A, Blackstone Point and B, section 2a at Grubbins Wood. Metre levels in relationship to the logs (SI Fig. S7, Fig. 3) are also shown. In both the extent of exposure of the Red Hill Limestone Formation is sand/mud-cover and tide dependent.

wet weather. For mapping purposes the member commonly occupies low flat, hummocky ground below and at the foot of the often scarp-forming upper Raven's Member. Other outcrops of the member are detailed in Table 1 and SI Table S1.

3.2. Raven's Member

The Raven's Member is 24–41 m thick. The member rests conformably on the Blackstone Member throughout the region, notably

at Coastguard Quarry and in the *type section* at White Scar Quarry (Figs. 3–6, 8B). The unit is rather heterogeneous but is dominantly comprised of dark grey to pale grey grainstones and packstones (Figs. 3, 9), with minor argillaceous interbeds, and occasionally sandy limestones and rare thin and sometimes channelised sandstones. Dolomitised units can make a significant component of the member, especially in outcrops around the Leven Estuary (e.g., Barker Scar, Low Frith, Figs. 3, 7, 9, SI Figs. S5, S6, S8), and Furness Peninsula (e.g., Nicholas, 1968), but also sometimes further east.



Fig. 5. The Blackstone Member–Raven's Member boundary at: A, Blackstone Point and B, section 2b at Grubbins Wood (between blue arrows). Metre levels in relationship to the logs (SI Fig. S7, Fig. 3) are also shown. Persons for scale in both photos. (For interpretation of the references to colour in this figure legend, the reader is referred to the web version of this article.)



Fig. 6. The Blackstone Member–Raven's Member boundary at: A) Coastguard Quarry and B) sub-section 1 at White Scar Quarry (see SI Fig. S3). In A) metre levels in relationship to the log (SI Fig. S7, Fig. 3) are also shown for stratigraphic scale.

Sections in the Arnside–Silverdale region are poor to absent in dolomitised beds.

In the mid-part of the member is a thin siliciclastic-rich unit (Fig. 3), which appears to be a useful marker for within-member correlation. At White Scar Quarry, this 0.4-m thick interval consists of shale, with minor sandstone (13.6–14.0 m; Figs. 3, 8B, 10A) and has bentonitic layers (which act as a spring seep). This is probably equivalent to a 1-m thick shale + bentonitic interval at Barker Scar (6–7 m, top bed A, Fig. 9), probably an unexposed interval (0.7 m) at Blackstone Point (20.5–21.2 m, Fig. 3), and a water-seep level in Heaves Quarry (Fig. 2, SI Table S1). In the Leven Estuary sections at Low Frith and Barker Scar, this mid-siliciclastic unit is associated with channelised limestone beds and channel features (SI Fig. S8).

The top ca. 1 m of the Raven's Member is rather heterogeneous in character and tends to be rich in fine-grained siliciclastics (Fig. 10A, C, D). This top siliciclastic-rich unit is best seen at Barker Scar, where it is rich in sandstone (bed E) and shale with some bioclastic limestone (beds F to G; Fig. 9, 10D). At White Scar Quarry, this top siliciclastic unit is largely shale and mudstone (in part bentonitic; Figs. 3, 9, 10C), with the lower part showing mottling (a weakly developed gleyed-palaeosol), and laterally impersistent sandstones (Fig. 3). Outside of man-made exposures (and Barker Scar) this top siliciclastic-rich unit of the member is normally covered or eroded, such as at the boundary interval at Grubbins Wood 1 and Sandside Railway cutting sections (Fig. 2, SI Figs. S2, S9). This, and the overlying lowest few metres of the Park Limestone, often forms the dip-slope depression between the resistant underlying Raven's Member limestones and the overlying more resistant lower ~10 m of the Park Limestone (as in Grubbins Wood, Fig. 9, SI Fig. S2). The sand-rich palaeosol inferred by Johnson et al. (2001) in the Canal Foot Quarry section (Fig. 2) relates to this top siliciclastic unit. The top of the Raven's Member is defined where the top siliciclastic unit (top of bed G at Barker Scar; Fig. 10D), passes up to non-argillaceous grainstones or dolomites, or sandy packstone–grainstones of the Park Limestone Formation (Figs. 3, 10B). In areas where this Raven's Member forms a distinct scarp-like feature, the

lowest parts of the Park Limestone are often scree covered, or form a flat-ledge on the underlying units.

3.3. Dalton Formation boundary changes

The lower boundary of the Dalton Formation proposed by Johnson et al. (2001) is not a viable, regionally-relatable feature since: 1) the section in the road cutting NE of the Elliscales Quarry (in Dalton in Furness; Fig. 2) is no longer exposed; 2) it is evident that a formation boundary at the position proposed by Johnson et al. (2001) now has no type section; and 3) the lithology and bedding character of strata underlying the Blackstone Member are typical of the Red Hill Limestone type lithology of the Furness Peninsula. We specifically examined the Low Frith section (Figs. 2, 7, SI Figs. S5, S6, S8) to evaluate the 'lower' division of Johnson et al. (2001). The Cat Cragg section (Figs. 2, 7) is located immediately below or at the base of the '*Chonetes carinata* Subzone, a feature which has guided prior divisions (Fig. 1). If there is a viable lithostratigraphic division near the basal "*Ch.*" *carinata* level, a more detailed regional evaluation is required of the Red Hill Limestone Formation—work which is currently ongoing.

In a break from previous placements of the base of the Park Limestone Formation, based on the nature of limestone colour change (Rose and Dunham, 1977), jointing-bedding (Johnson et al., 2001), or biostratigraphy at Barker Scar (Ramsbottom, 1981), we have used the argillaceous nature of the uppermost part of the Raven's Member (top is bed G at Barker Scar; Fig. 10D) to distinguish it from the overlying non-argillaceous Park Limestone (base is bed H at Barker Scar). This is a more robust and precise means of defining this formational boundary in well exposed outcrops, but it does not negate the use of the 'typical' style of jointing and poorly-developed bedding, which allows the Park Limestone to be normally distinguished in poorer outcrops. Unfortunately, such 'typical' bedding features are not universal throughout the Park Limestone Formation, as evident by the erroneous formation boundary placement of Balderstone and Dewey (2003), as noted above. Recently, Waters et al. (2021) proposed to reposition of the

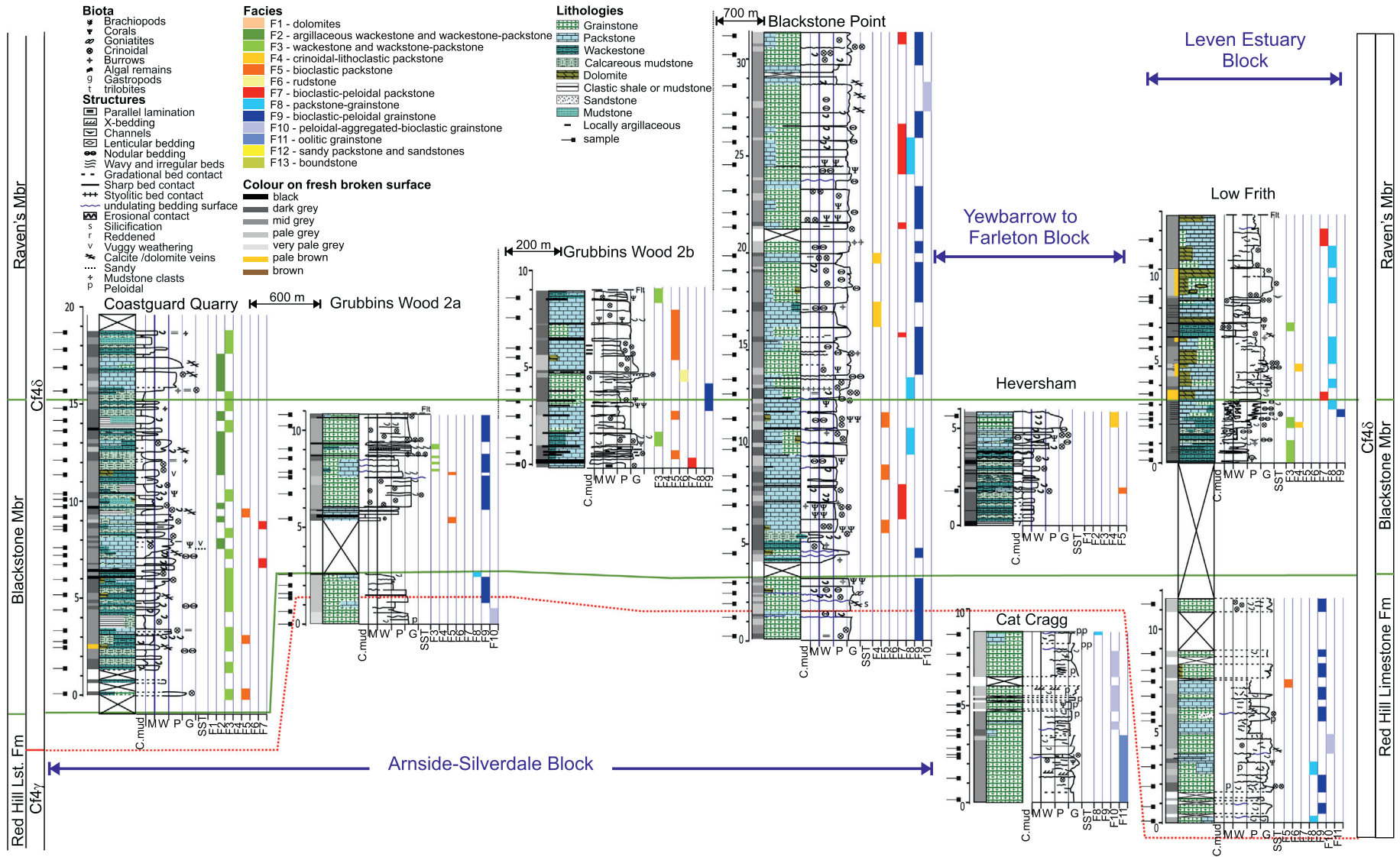


Fig. 7. Correlation of the sections involving the boundaries (in green) of the Blackstone Member and the underlying Red Hill Limestone Formation. The 'blocks' relate to the outcrop regions in Figure 2. Distance between sections shown. The base of the C146 subzone shown in red. Microfacies divisions shown for sampling points (pointer symbol). For detailed sample number data see the Supplementary information. (For interpretation of the references to colour in this figure legend, the reader is referred to the web version of this article.)

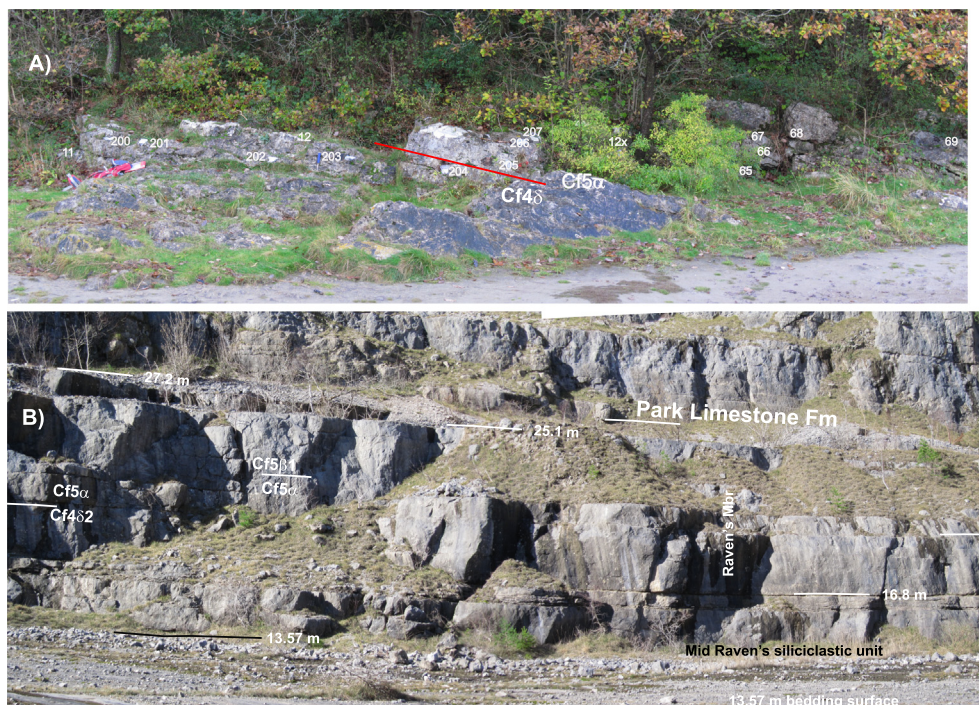


Fig. 8. The upper part of the Raven's Member at: A) Grubbins Wood section-1 across the Arundian–Holkerian boundary (hammer and rucksack for scale) and B) sub-section 2 at White Scar Quarry (metre levels for scale). See also Figures 3, 9 and SI Figures S2, S3, S9. In B) the Park Limestone Formation continues into the overlying cliff (some 65 m high).

base of the Park Limestone Formation at bed P at Barker Scar, due to the occurrence of an unconformity at the base (unrecognised by us) and the occurrence of the rugose coral *Lithostrotion araneum* (late Holkerian). However, this level is not regarded herein to be a reliable or mappable feature for the base for the Park Limestone, since it is located in the middle of pale grey grainstone facies (SI Fig. S8), macrofauna in most sections are scarce and the unconformity is questionable and not recognised in any previous studies.

4. Zircon and apatite U–Pb geochronology from the bentonites

Bentonitic samples WSB1 to WSB5 were collected from six levels in the Raven's Member mid and top siliciclastic units at White Scar Quarry (details in Fig. 10A, C). Only two zircons (from WSB-3 and WSB-4) and two apatites (both from WSB-2) yielded ages within uncertainty, of the likely stratigraphic age (out of 439 and 75 analyses respectively, Fig. 11) and hence the zircon and apatite U–Pb populations are regarded as nearly entirely detrital in origin. The zircon (U–Pb concordia ages) and apatite (^{207}Pb -corrected ages) U–Pb data from the five samples combined are plotted together in Figure 11. The zircon data exhibit peaks at 425 Ma, 950 Ma–2050 Ma (with prominent peaks at 1050 Ma, 1500 Ma and 1700 Ma), 2750–2850 Ma and 3650 Ma. Importantly, they contain very restricted detritus at 550–650 Ma and none at 2200 Ma. These latter age peaks are highly diagnostic of an Avalonian source or other peri-Gondwanan terranes such as Iberia or Armorica (Pointon et al., 2012). Instead, nearly all the zircons and apatites are consistent with an ultimate source in Laurentia. They closely resemble U–Pb detrital zircon spectra from the Ordovician successions of the Southern Uplands, which are in turn sourced from the Laurentian hinterland (Waldron et al., 2008), with the addition of a prominent ca. 425 Ma peak likely derived from the voluminous Devonian granites emplaced into the Southern Uplands terrane. The apatite U–Pb data are dominated by a similar (ca. 410 Ma) Devonian granite peak (Fig. 11), likely derived from the Southern Uplands terrane, but also a minor amount of 2300–2700 Ma detritus. The only plausible source for the 2300–2700 Ma apatite peak

is the Lewisian Complex of NW Scotland (or its equivalents in SE Greenland such as the Nagsugtoqidian Mobile Belt). As apatites more likely represent a first cycle mineral phase compared to zircon (Morton and Hallsworth, 1999), it implies that there is likely a component of first-cycle sourcing from these early Paleoproterozoic–late Archean terranes into the Dalton Formation.

There is an abundance of provenance data for the Namurian, Millstone Grit Group (MGG) of the Pennine Basin (see summaries in Lancaster et al., 2017 and Chew et al., 2020). Critically, these multi-proxy datasets include both refractory mineral phases that are prone to recycling (the U–Pb zircon system) and labile first-cycle provenance proxies (Pb-in-K-feldspar analyses, Tyrrell et al., 2006), and are thus more provenance diagnostic than studies on Carboniferous basins of northern England, which rely mainly on U–Pb detrital zircon data (e.g., Morton et al., 2021).

These comprehensive multi-proxy datasets show that sand in the northern parts of the Pennine Basin system in the Namurian was derived from two major sources – the Archean–Paleoproterozoic of NW Scotland (or the equivalent Nagsugtoqidian in SE Greenland) and the Southern Uplands terrane and its suite of Caledonian granites, although the relative importance of the Southern Uplands terrane as a source is debated (Tyrrell et al., 2006; Lancaster et al., 2017). A similar sediment routing system (Archean–Paleoproterozoic of NW Scotland or equivalents in SE Greenland and the Southern Uplands terrane) is envisaged here for the Dalton Formation. Comparing the U–Pb zircon spectra of the MGG from the northern part of the Pennine Basin with the U–Pb zircon and apatite spectra from the White Scar Quarry samples (Fig. 11), the Archean peak in the samples is much smaller and the amount of Proterozoic zircon (recycled from the Southern Uplands terrane) is enhanced. This suggests that in the late Arundian the Southern Uplands were more topographically enhanced compared to the later Namurian, and so the Southern Uplands acted as more of a barrier to fluvial transport from the Archean gneisses of the Laurentian hinterland to the north. This provenance scenario is compatible with sediment routing system reconstructions in both the Tournaisian and Viséan successions

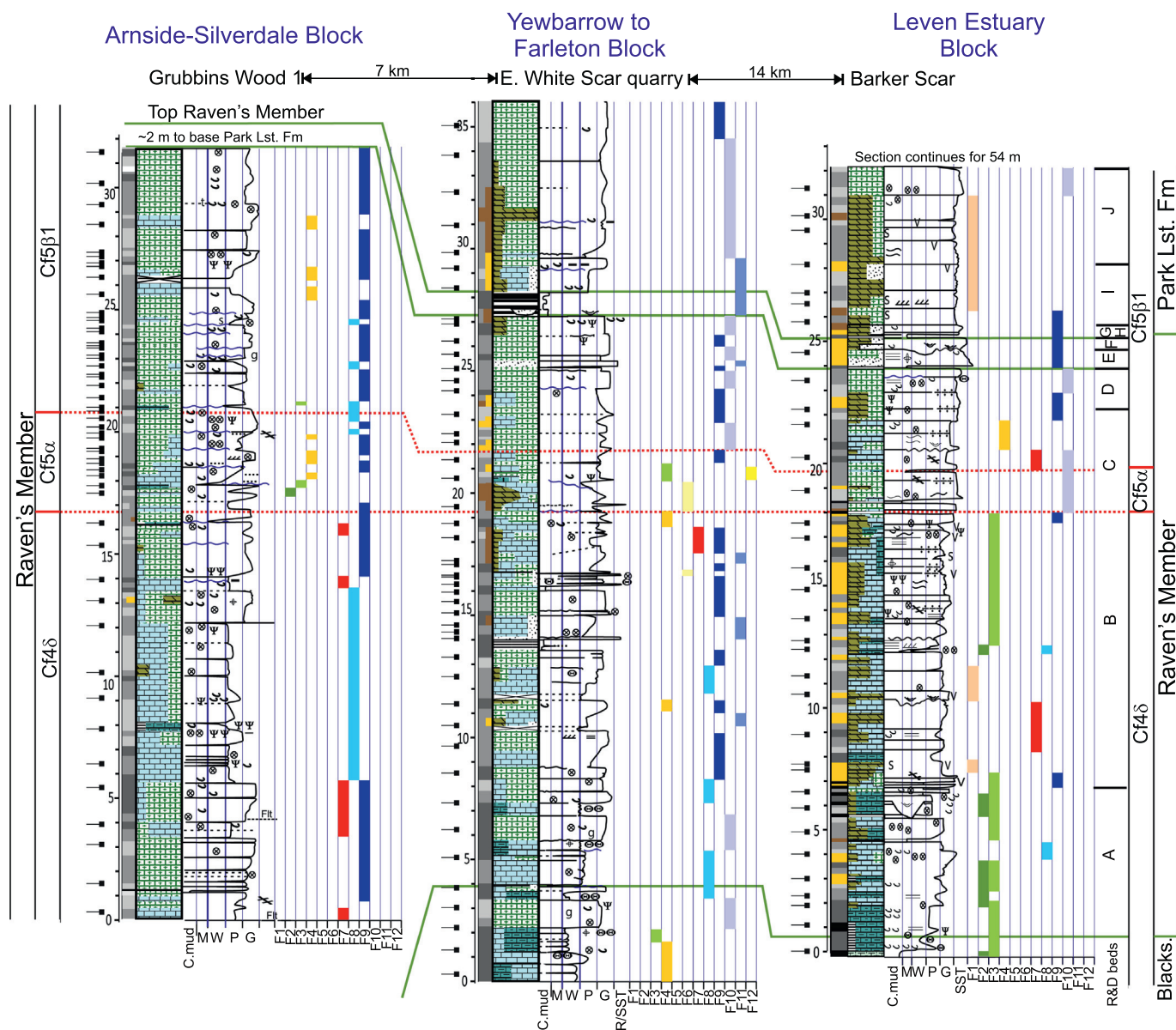


Fig. 9. Correlation and microfacies of the sections at Grubbins Wood-1, White Scar Quarry and Barker Scar, including the Raven's Member of the Dalton Formation and the lower part of the Park Limestone Formation. Legend in Figure 7. Foraminifera subzone boundaries in red, lithological ones in green. R&D beds = Rose and Dunham (1977) bed letters at Barker Scar. (For interpretation of the references to colour in this figure legend, the reader is referred to the web version of this article.)

of the Solway and Northumberland basins (Leeder, 1974; Maguire et al., 1996), which indicate palaeoflow from both the Southern Uplands, and NE-sourced fluvial systems, which were ultimately derived from north of the Scottish Caledonides.

5. Microfacies

From analysis of thin sections under the petrological microscope, twelve limestone facies (F2–F13) have been distinguished in the sections, along with dolostone (F1) (Figs. 7, 9, 12), from which the main environments recognised are summarised in Figure 13.

5.1. Dolostone (F1)

Crystalline dolostone is characterised by inequigranular, non-rhombic, tightly packed dolomite crystals of microcrystalline dolomite (micrite sized) and rarely euhedral or subhedral with microcrystalline centres, with sizes > 40 µm. Crystals are curved or lobate. Small amounts of clay also occur between grains.

Sampled dolostones are only present in the Barker Scar section, in both the Dalton Formation (Raven's Member) and Park Limestone Formation (Figs. 9, 12).

5.2. Argillaceous wackestone and wackestone–packstone (F2)

Argillaceous wackestone facies are predominant, but in some cases, horizons are richer in bioclasts, and thus intermediate wackestone–packstone textures are also common (Fig. 14A). Variations in skeletal content occur in bands. The percentage of micrite varies mostly between 40% and 50% (rarely up to 70%), and non-skeletal components are mostly quartz grains, lithoclasts and peloids. Skeletal components show a great diversity, including commonly crinoids, foraminifers, brachiopods, ostracods, donezellids (*Kamaenella*), palaeoberesellids (*Kamaena* and *Palaeoberesella*), molluscs (gastropods and bivalves) and dasycladaceans (*Koninckopora* and *Nanopora*). Comparatively, the proportion of crinoids is low compared to other microfacies (10–20%, rarely up to 35%), but noteworthy, is the high percentage of foraminifers in some beds (up to 20%). Usually, clasts are poorly sorted, but rarely a

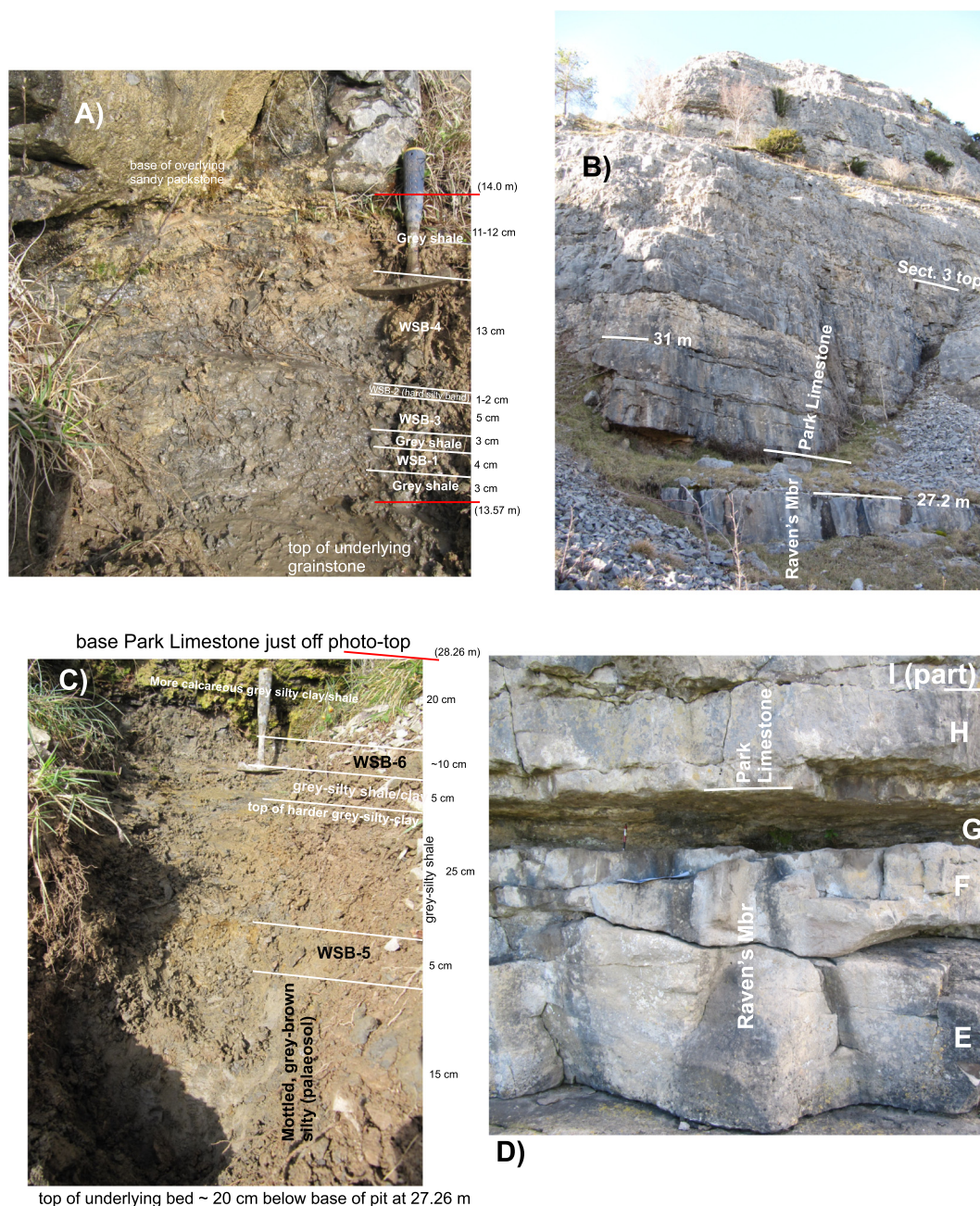


Fig. 10. A, The mid siliclastic unit (Raven's Member) in White Scar Quarry from an excavated part of sub section-2, with location of samples WSB1–WSB4 (see SI Fig. S3) used for zircon and apatite U–Pb dating. B, Boundary of the Raven's Member (Dalton Formation) and Park Limestone Formation in White Scar Quarry, sub section-3 (SI Fig. S3). C, Close-up view of top siliclastic unit (Raven's Member, sub section-2) and location of samples (WSB-5 to WSB-6) for the detrital zircon and apatite study (thicknesses in cm, metre levels in Fig. 3). Metre levels in relationship to the logs (Fig. 3) are also shown for stratigraphic scale. D, Boundary interval of the Raven's Member and Park Limestone Formation at Barker Scar, labelled with bed codes of Ramsbottom (1981). Pencil for scale. Here beds E, F, and G represent the top siliclastic unit of the Raven's Member (Fig. 9).

moderate sorting is observed. Elongated bioclasts tend to be well-oriented and parallel, wavy and cross-laminated parts are present. Bioclasts are usually broken. Partial dolomitisation is present in about half of the samples, usually affecting the most argillaceous parts. Bioturbation occurs, but it is not particularly abundant.

This facies is present in the Blackstone and Raven's members (Dalton Formation; Fig. 12) of the Coastguard Quarry and Barker Scar sections, but only at the top of the Raven's Member in the Grubbins Wood 1 section (Figs. 7, 9).

Interpretation: Predominance of muddy material suggests that conditions correspond to the background sedimentation on a ramp below fair-weather wave-base (FWWB). The banding caused by concentrations of bioclasts, laminations and orientation of

elongated bioclasts, suggest alternation of low-energy and high-energy hydrodynamic conditions, inferred to be sporadically storm-induced and so depths are implied above the storm wave-base (SWB). Bioclastic diversity is high and composed of stenohaline organisms typical of normal marine, open sea neritic shelves. The amount of mud in suspension in the environment and the abundance of palaeoberesellids and donezellids suggest a primary turbid environment, mostly dysphotic, although it alternates rarely with levels with abundant green algae and foraminifers, suggesting local minor levels with euphotic conditions (Cózar et al., 2019). These features suggest that the facies accumulated in the deep subtidal part of the shelf (Fig. 13). This is comparable to Standard Microfacies (SMF 9) of Flügel (2004).

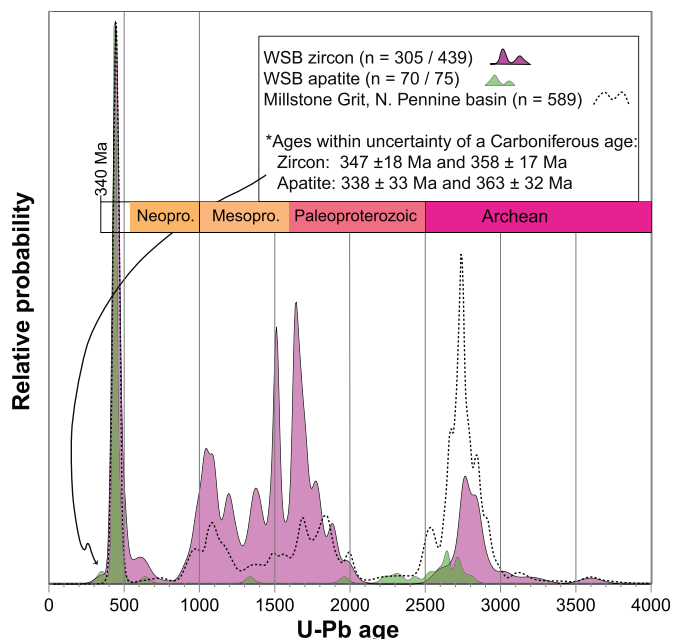


Fig. 11. Detrital zircon and apatite U–Pb ages (U–Pb concordia and ²⁰⁷Pb-corrected ages respectively) from the White Scar bentonites (WSB, Fig. 10). The number of grains that passed an age acceptance criterion (concordance *sensu stricto* for zircon and the age uncertainty threshold of Chew et al. (2020) for apatite respectively) are listed along with the total number of grains analysed. U–Pb detrital zircon spectra from the Millstone Grit Group of the northern Pennine Basin are also provided for comparison— from the literature sources cited in Lancaster et al. (2017) and Chew et al. (2020). To aid direct comparison between the different datasets which have substantially different amounts of grains analysed, all datasets were scaled relative to the Devonian age peak.

5.3. Wackestone and wackestone–packstone (F3)

This facies contains similar percentages of matrix and components (F3 part of Fig. 14B) as in facies F2. However, lithoclasts and peloids are more abundant, whereas quartz grains are rather scarce. Furthermore, the percentages of foraminifers have notably decreased (as well as ostracods), but crinoids in comparison to F2 have increased. This facies shows largely poorly-sorted components, rarely moderately-sorted, with a high degree of fragmentation and oriented bioclasts (parallel and wavy orientation). Bioturbation is negligible, except in some rare samples. Dolomitisation is more common than in the argillaceous wackestones, which indistinctly effects both the matrix and components. There is no marked banding in concentrated bioclastics.

This facies is mostly present in the Dalton Formation (commonly in the Blackstone Member at Coastguard Quarry and Raven’s Member at Barker Scar sections and in both members at the Low Frith section; Fig. 12). One sample of the Park Limestone Formation is assigned to this facies (sample BS55 at 47.1 m, from C  zar et al., 2022; see Supplementary data).

Interpretation: Owing to the similar components and textures, this microfacies is comparable to F2, and so also interpreted as from the outer shelf below FWWB and SWB (Fig. 12C), very rarely affected by storms, within normal marine open sea conditions that are predominantly dysphotic. However, the higher amount of bioclasts suggests more proximal positions on the shelf. This is comparable to Standard Microfacies (SMF 9) of Fl  gel (2004).

5.4. Crinoidal–lithoclastic packstone (F4)

This facies contains common lithoclasts of varied sizes (including common micro-intraclasts, *sensu* Fl  gel, 2004) and crinoids (Fig. 14C). Micrite is less than 30% and locally the matrix is argillaceous. Other important bioclasts are brachiopods, foraminifers, ostracods and

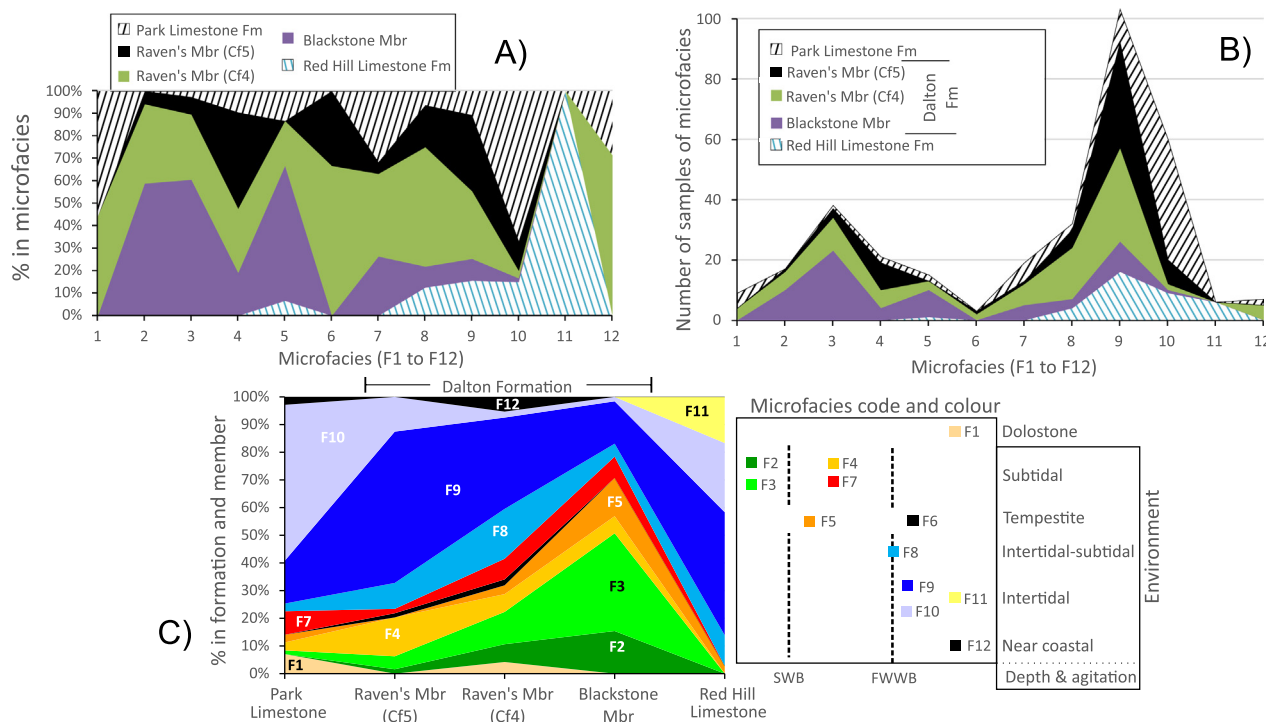


Fig. 12. Summary of the distribution of microfacies with respect to the formations and members. The Raven’s Member is subdivided into two units belonging to the Cf46 and Cf5α–β1 zones. A, the facies abundance expressed as a percentage of the total for each microfacies and; B, as the total number of samples. C, The distribution of microfacies with respect unit divisions, as a percentage of the total number of samples from those units, and a summary of the inferred environmental subdivisions with respect to microfacies. Data also includes the entire dataset from the Park Limestone Formation at Barker Scar of C  zar et al. (2022).

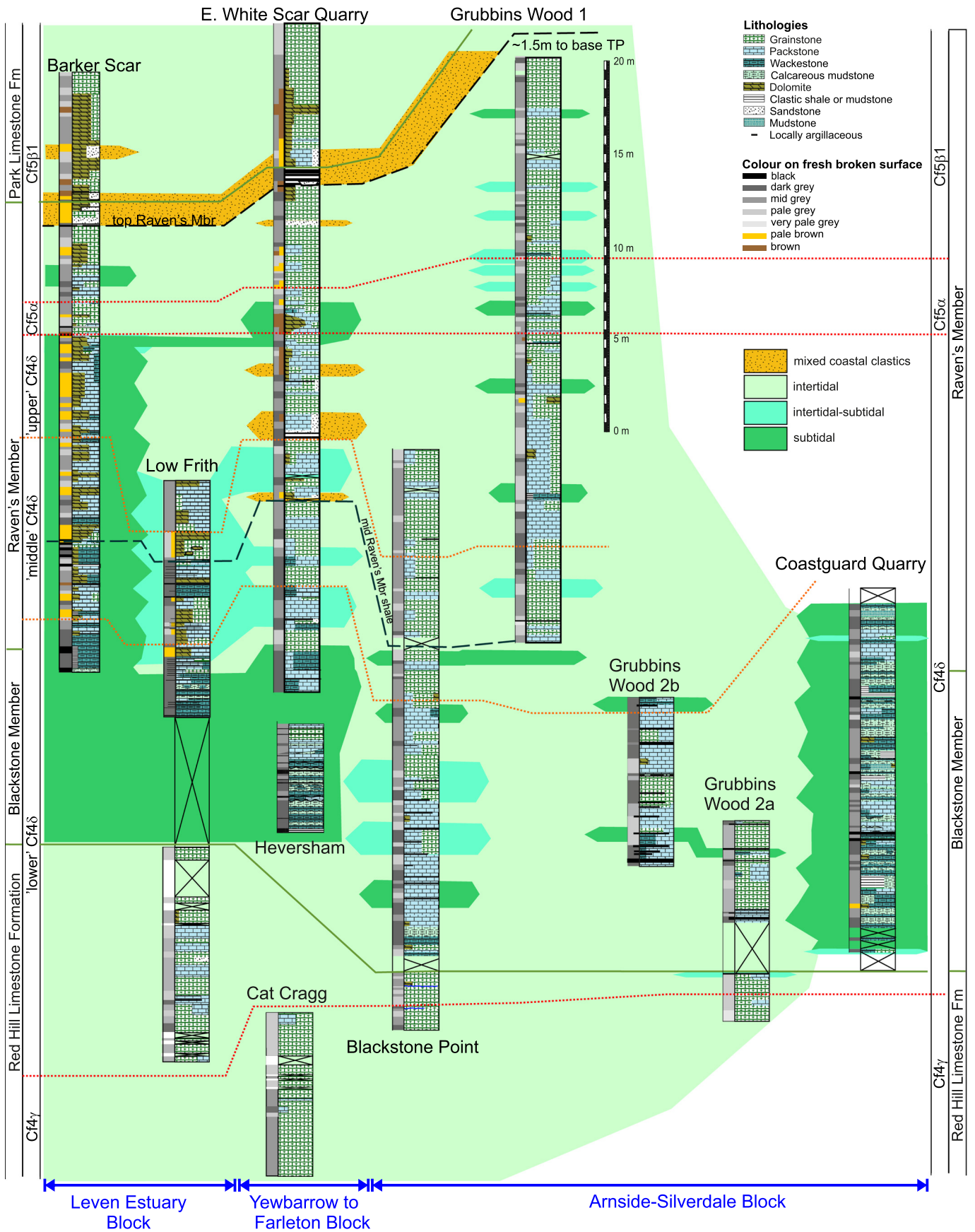


Fig. 13. Environmental interpretation of the studied sections based on the microfacies. The foraminiferal subzonal boundaries shown in red, the three informal subdivisions of the Cf46 subzone shown in orange, lithostratigraphic boundaries in green and siliciclastic unit correlations shown as black dashed lines. The 'blocks' relate to outcrop regions in Figure 2, but columns are not geographically distributed. (For interpretation of the references to colour in this figure legend, the reader is referred to the web version of this article.)

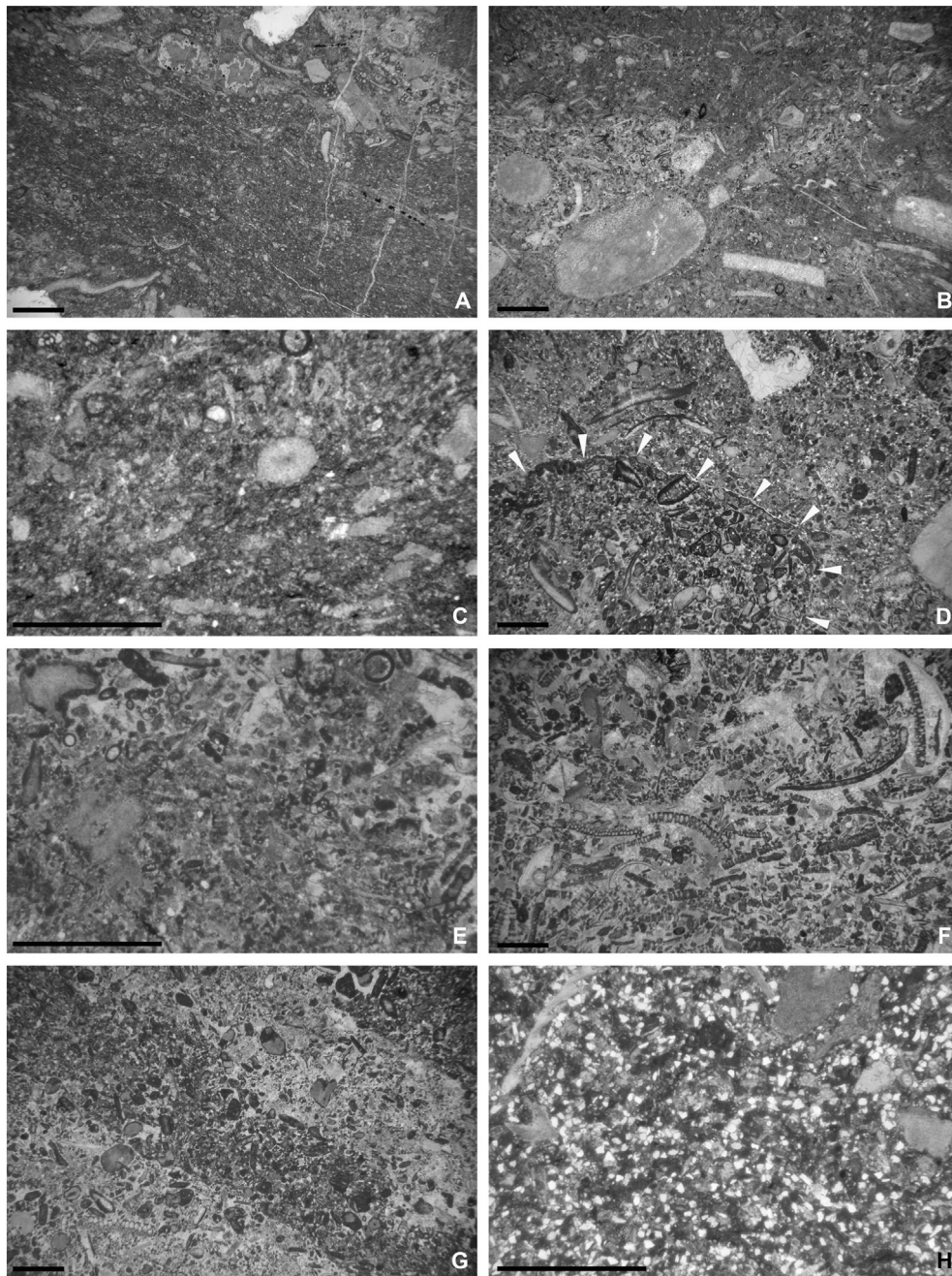


Fig. 14. Main types of microfacies (scale bar 2 mm). A, Argillaceous wackestone (F2) passing upward to bioclastic packstone rich in crinoids (partly silicified) and foraminifers (F7). Note that the base is also richer in bioclasts, some with pyrite—sample CG24. B, Bioclastic packstone (F5) passing upward to wackestone (F3)—sample CG1. C, Crinoidal-lithoclastic packstone (F4)—sample BP17. D, Rudstone (F6). Note the large bioclastic grainstone pebble on the lower left (indicated by arrows)—sample WS25. E, Crinoidal-foraminiferal packstone-grainstone (F8). The upper part contains more cements—sample GW9x. F, *Koninckopora*-peloidal grainstone with abundant aligned green algal stipes (F9)—sample WS37. G, Peloidal-aggregates grainstone (F10). Banding is related to concentrations of aggregates (dark bands), and bands with less aggregates and a higher percentage of cement—sample WS36. H, Sandy packstone with abundant angular silt-size quartz grains (F12)—sample WS15. See Supplementary information for precise sample location and petrographic details.

dasycladales, but compared to the F3 microfacies abundances are lower. Furthermore, the overall diversity of bioclasts is much lower than in facies F3, and rarely molluscs, donezellids, oujgaliids, bryozoans and trilobites are recorded. Components are poorly sorted, although some parallel orientation of brachiopods is observed. The degree of fragmentation is very high. Micritisation of grains along with coating processes is recognised.

This facies is present in both the Blackstone and Raven's members in many sections (Fig. 12), except for the Coastguard Quarry and Grubbins Wood 2a and 2b sections (Figs. 7, 9).

Interpretation: Conditions correspond to sedimentation on a ramp above storm wave-base (SWB) with productive tempestites. The stenohaline bioclastic diversity of the transported material suggests normal marine open-sea conditions. This is comparable to Standard Microfacies (SMF 4 and SMF10) of Flügel (2004).

5.5. Bioclastic packstone (F5)

The predominant components are crinoids or palaeoberesellids/donezellids and sometimes common lithoclasts and foraminifers

(Fig. 14B). Brachiopods usually occur, but never in abundance and foraminiferal diversity is very low. Sorting is moderate to high, with many fragmented bioclasts and usually palaeoberesellids are strongly oriented (in parallel, wavy and cross-laminations). The amount of micrite in the matrix is less than 30% and the components are densely packed.

This facies is only present in the lower part of the Dalton Formation at Coastguard Quarry, Blackstone Point and Grubbins Wood 2a and 2b sections (Fig. 7). One sample is present in the Red Hill Limestone Formation at Low Frith (Fig. 12).

Interpretation: Tempestites formed in conditions similar to those for microfacies F4.

5.6. Rudstone (F6)

This is characterised by pebbles of typical bioclastic–peloidal grainstone derived from facies F9 (Fig. 14D). Some clasts reach up to 1 cm in diameter, and are embedded in a matrix composed of crinoid, brachiopod or palaeoberesellid packstone, generally with a strong fragmentation, but also highly packed fragments. Other components are negligible, except for the occurrence of quartz grains.

This facies is rare and is only observed in two levels of the Dalton Formation (Raven's Member) in White Scar Quarry and Grubbins Wood 2b sections (Figs. 7, 9, 12).

Interpretation: Conditions seem to correspond to sedimentation on a shelf above storm wave-base (SWB) with active storm deposits. These tempestites (grainstone facies) developed in intertidal conditions, eroding and transporting the boulders to near-shore locations. This is comparable to Standard Microfacies (SMF 4) of Flügel (2004).

5.7. Bioclastic–peloidal packstone (F7)

Peloids are the result of micritisation and are not the result of small micritic intraclasts (micro-intraclasts). Crinoid and peloid contents both range from 40% to 60%. The micrite content is less (usually less than 20% abundance) than in the F4 and F5 packstone facies, with all the skeletal and non-skeletal components densely packed, with many sutured interparticle contacts (Fig. 14A). Brachiopods are an important skeletal component, as well as dasycladales, whereas the percentage of foraminifers is notably increased—in some samples up to 15% in abundance. The diversity of other bioclasts is poor and with lower abundances. In contrast to most of the previous facies, sorting is moderate, with rare parallel orientation of bioclasts, with a high degree of fragmentation. Micritisation of grains and coatings are common. The abundance of peloids and crinoids increases in samples which show well-sorted patches, with spar instead of micrite in the matrix. Bioturbation is common and locally recrystallization of the micrite to equant spar, gives the false appearance of a grainstone, not in stratified areas but in bioturbated patches.

This facies occurs mostly in the lower to mid parts of the Dalton Formation in both of its members (Figs. 7, 9), but also in the Park Limestone Formation (Fig. 12).

Interpretation: Micrite in the matrix suggests the background sedimentation was in subtidal settings, below FWFB. The fragmentation, variable sorting, lamination and high packing in this facies suggest that deposits were frequently affected by storms, and thus, this microfacies facies is inferred to be formed between the FWFB and SWB. There is a variety of stenohaline fauna typical of normal marine conditions. The common micritisation processes and dasycladales are interpreted as representative of euphotic conditions. This is comparable to Standard Microfacies (SMF 4 and SMF10) of Flügel (2004).

5.8. Packstone–grainstone (F8)

Peloids are common and usually 10–20% in abundance (but range up to 25%), along with crinoids. Although these two components are the most abundant in facies F8, they are present in lower percentages

compared to other microfacies (Fig. 14E). Compared to other facies the abundance of other bioclasts is significantly increased (*i.e.*, bioclasts such as foraminifers, brachiopods, dasycladales, molluscs and ostracods). Some samples have many calcispheres and locally oncoids, although the overall bioclast diversity is low. The percentage of spar and micrite varies but together represents 20–30% by area. Sorting of the components is usually moderate, with a moderate packing and a high degree of fragmentation. Bioturbation rarely occurs, and only one sample shows clear parallel lamination.

This facies is common in the Dalton and Red Hill formations in the Grubbins Wood 1 section as well as in the Low Frith sections. It occurs less so in the Dalton Formation at Blackstone Point and Barker Scar (Figs. 7, 9, 12).

Interpretation: Shoals close to the FWFB which locally inhibited micrite preservation, to be washed away in fluctuating intertidal to subtidal normal marine conditions under euphotic conditions. This is comparable to Standard Microfacies (SMF 13 and SMF16) of Flügel (2004).

5.9. Bioclastic–peloidal grainstone (F9)

This is the most common facies, which also has a moderate diversity of bioclasts (Figs. 12B, 14F). Micritised elements (peloids) usually range from 15% to 50% in abundance. Two samples of F9 facies do not contain peloids, but instead mostly contain crinoids and brachiopods. Common components are crinoids, foraminifers and brachiopods, with a larger percentage of foraminifers in some beds (up to 20%). Other common bioclasts include dasycladales, molluscs and ostracods. These components are usually moderately sorted, and in some cases well-sorted, with a high degree of fragmentation. Bioturbation occurs but it is not a dominant feature. Micritisation of grains and coatings are common and aggregate grains can occur in abundance, but only in three samples. Components show a low to moderate packing and the abundance of cement varies between 30 and 40%. The most unusual samples are rich in *Koninckopora* (sample WS-37 and WS-39; Fig. 3) showing some alignment of *Koninckopora* (Fig. 14F) or contain *Luteotubulus liscis* (Malakhova, 1975) (sample WS-48) with rare rugose and tabulate corals.

This facies occurs commonly only in the Dalton Formation (Blackstone and Raven's members; Fig. 12) at Grubbins Wood 1 and 2 sections, at White Scar Quarry, Low Frith and Blackstone Point sections (Raven's Member), but more rarely at Barker Scar (Figs. 7, 9). It is also common in the Park Limestone Formation at White Scar Quarry and Barker Scar (Figs. 9, 12A). It is the dominant facies in the Red Hill Limestone Formation at the Blackstone Point and Grubbins Wood-2a sections (Figs. 12B, 7).

Interpretation: Shoals above the FWFB in intertidal normal marine euphotic conditions. This is comparable to Standard Microfacies (SMF11 and SMF16) of Flügel (2004).

5.10. Peloidal–aggregate–bioclastic grainstone (F10)

This is the second most abundant facies (Fig. 12B) and is distinguished from the F9 grainstone facies by the amount of aggregated grains, which together with the peloids show a rather similar or higher abundance to the sum of the skeletal components (Fig. 13G). Skeletal components show a low diversity with the most abundant (in decreasing order) being crinoids, brachiopods, dasycladales, foraminifers and molluscs. Importantly, there is a lower abundance of foraminifers and a higher abundance of dasycladales compared to the F9 grainstone facies. Donezellids also become common in some beds, although they occur in most samples with low percentages. Sorting is moderate to high, but only rarely is parallel lamination observed. Components show a low packing density, with cement content greater than 30%, and rarely at a moderate level. The degree of fragmentation is large and micritisation and coatings are common.

This facies is common at Barker Scar, White Scar Quarry and Low Frith sections, mostly (but not exclusively) from the Raven's Member

and Park Limestone Formation (Fig. 12). Rarer samples assigned to this facies are also present at Blackstone Point (Raven's Member, one sample), as well as in the Red Hill Limestone Formation in the Grubbins Wood 2a and Cat Cragg sections (Figs. 7, 9).

Interpretation: changing energy conditions close to shoals above the FWWB in intertidal settings, but generally slightly lower energy than the bioclastic–peloidal grainstone facies F9. This facies is comparable to Standard Microfacies (SMF17 and SMF18) of Flügel (2004).

5.11. Oolitic grainstones (F11)

This facies is characterised by the abundance of ooids ranging upwards from 25% (but generally 40–65%), with common mud aggregates and bioclasts. Ooids are always of small size, rounded to egg-shaped, commonly less than 200 µm in diameter, and composed of mostly superficial ooids yielding only 1 or 2 laminae with radial fabrics (ca. 25 to 40 µm in total thickness). Mature ooids composed of multiple laminae are not observed. Bioclasts unaffected by coatings are scarce, most frequently crinoids and brachiopods, as well as rare foraminifers, ostracods and dasycladales.

The facies is only recorded in the lower part of the Cat Cragg section (Red Hill Limestone Formation; Figs. 7, 12).

Interpretation: high-energy shoals above the FWWB, comparable to Standard Microfacies (SMF15) of Flügel (2004).

5.12. Sandy packstone and sandstone (F12)

The quartz grains are always immature with a dominance of angular morphologies, with more rarely subangular shapes (Fig. 14H). Their size depends on the particular sample, because they are usually very well-sorted, with grains < 50 µm in some, or up to about 150 µm in other samples. In addition to quartz grains, the microfacies contains crinoids, brachiopods and ostracods, as well as lithoclasts (from microlithoclasts to larger sizes). This facies generally displays a moderate to high degree of sorting of all components, forming a mixture of typical skeletal and non-skeletal components, including, more rarely, low percentages of dasycladales, molluscs and bahamites. Wavy to parallel laminations occur.

Quartz grains are also rather common in all other facies particularly in sections such as Grubbins Wood (ranging 1% to 5%, rarely 10% and 15% in abundance), Blackstone Point (1% to 5%), and Barker Scar (1% to 5%, rarely 10% and 15%). However, in the White Scar Quarry section quartz grains are more abundant in many beds (reaching 10% to 20%), but also in sandier lithologies reaching up to 30–40% quartz and up to 80% in one sample, which is considered a sandstone.

This microfacies is virtually restricted to the White Scar Quarry section, from the upper Dalton Formation (Raven's Member) and Park Limestone Formation (Figs. 9, 12A).

Interpretation: near-coastal siliciclastic–carbonate margin.

5.13. Boundstone (F13)

Only one type of boundstone has been recognised, which is White Scar Quarry sample WS-30 (Raven's Member) (Fig. 3), where there is a bafflestone (partly a framestone) composed of a small bioherm of the tabulate coral *Syringopora*, in which between the corallites is a poorly fossiliferous micrite matrix (wackestone) with rare peloids, brachiopods and foraminifers. In the upper part, this bioherm passes into a packstone facies rich in broken and accumulated *Koninckopora*, which originally could have constituted a bafflestone texture.

Interpretation: subtidal, below SWB and FWWB. This is closely comparable to Standard Microfacies (SMF 7) of Flügel (2004).

6. Foraminiferal biostratigraphy

Conil et al. (1980) divided the Arundian into early (Cf4β subzone), middle (Cf4γ) and late (Cf4δ) subzones. According to Riley (1993) the

late Arundian is equivalent to the S1 macrofossil division (i.e., Gastropod Beds; Fig. 1) of Garwood (1913). The most important foraminifers of the Cf4δ subzone are illustrated in Figures 15 and 16. Those for the Holkerian Cf5α and Cf5β subzones are illustrated from the Barker Scar section in Cózár et al. (2022).

The Cf4γ subzone (mid Arundian) is represented in two levels in the lower part of the Blackstone Point and Grubbins Wood 2a sections, as well as in the entire Cat Cragg Quarry section (Fig. 7). This subzone is characterised by the occurrence of species of *Archaeodiscus* and *Lebedeva* in *involutus* stage *sensu* Pirlet and Conil, 1977 (e.g., *A. koltjubensis* Rauser-Chernousova, 1948c, *A. vischerensis* Grozdilova and Lebedeva in Dain and Grozdilova, 1953, *A. mohae* Conil and Lys, 1964, *A. piesis* Conil and Lys, 1964 and *A. pulvinus* Conil and Lys, 1964), as well as transitional forms between the *involutus* and *concauus* stages—the concept of *Archaeodiscus* and its evolutionary stages, as used herein, is discussed in Cózár and Somerville (2020). Based on studies from north Africa (e.g., Vachard and Tahiri, 1991; Cózár et al., 2020b), three further characteristic Cf4γ subzonal taxa are *Conilidiscus* sp., *C. settlensis* (Conil and Conil et al., 1980) and *C. bucculentus* (Conil and Lys, 1964), with the genus *Conilidiscus* a potentially worldwide marker for the Cf4γ subzone. Another key taxon is *Forschiella prisca* Mikhailov, 1939, defined as a marker for the Cf4γ subzone by Conil et al. (1980) and Pille (2008), who considered that the species might first occur from the Cf4β(?) Zone in Belgium, but reliably confirmed from the Cf4γ—although Kalvoda et al. (2011) recorded this species in the latest Tournaisian. However, the illustrated Tournaisian specimen (Kalvoda et al., 2011, fig. 11G) seems to be closer to *Alticonilites* (cf., *A. dinanti* (Conil and Lys, 1964)), a taxon first occurring from the latest Tournaisian. Thus, *Forschiella prisca* is considered also a valid guide for the Cf4γ subzone. This subzone is equivalent to the MFZ11β of Cózár et al. (2020a).

The base of the Cf4δ subzone is recognised in the topmost few metres of the Red Hill Limestone Fm in the Arnside shore sections (Figs. 1, 7)—at Blackstone Point and Grubbins Wood 2a sections. The subzone is also widely represented in the Coastguard Quarry and Grubbins Wood section 2b sections and basal samples in Grubbins Wood 1 (Figs. 7, 9). Compared to macrofossil zonations, the base of the Cf4δ subzone is somewhat older than previously thought, occurring within the upper part of the “Ch.” *carinata* Subzone of Garwood. In the Leven Estuary area, the upper part of the Red Hill Limestone Formation already yields foraminiferal markers of the Cf4δ subzone, but the older Cf4γ subzone has so far not been recorded in this area. Clearly, the base of the Blackstone Member is either; a) slightly diachronous, or b) the lower part of the Cf4δ subzone is condensed in the basal shales of the Blackstone Member in the Arnside area and is age-equivalent to the top of the Red Hill Limestone Formation in the Leven Estuary Area.

In the Yewbarrow to Farleton Block the Cf4δ subzone is recognised in the Heversham Railway cutting and the lower part of the White Scar Quarry section. The Cf4δ subzone also is recognised in the entire Low Frith section, as well as in the lower part of the Barker Scar section (Figs. 7, 9). The Cf4δ subzone is characterised by classical markers, including the first occurrence of *Cribranopsis* sp. 1 (a more evolved form than *C. fossa* Conil and Naum, 1976; Fig. 15B), *Latiendothyranopsis solida* (Conil and Lys, 1964) (Fig. 15C), *Endospiroplectamina syzranica* (Lipina, 1948) and primitive forms of *Nodosarchaediscus* (e.g., *Nodosarchaediscus? cornua* (Conil and Lys, 1964), *N.? viae* Vachard, 1977, *N.? sp. 1 sensu* Cózár et al., 2022; Fig. 16C–E) (Conil et al., 1980, 1991), as well as other markers proposed by Cózár et al. (2020a). These are *Lituotubella glomospiroides* Rauser-Chernousova, 1948a (Fig. 15A), large species of *Plectogyranopsis* (*P. moraviae* Conil and Longerstaey in Conil et al., 1980) and *P. settlensis* (Conil and Longerstaey in Conil et al., 1980; Fig. 15E–F), and *Omphalotis* aff. *minima* (Rauser-Chernousova and Reitlinger in Rauser-Chernousova et al., 1936) *sensu* Cózár et al. (2022) (Fig. 15I), a more primitive species than the nominal species. The assemblages seen here are of high diversity containing common taxa from the underlying Cf4γ foraminiferal subzone. These Cf4δ assemblages and markers are more frequent in the deeper-water

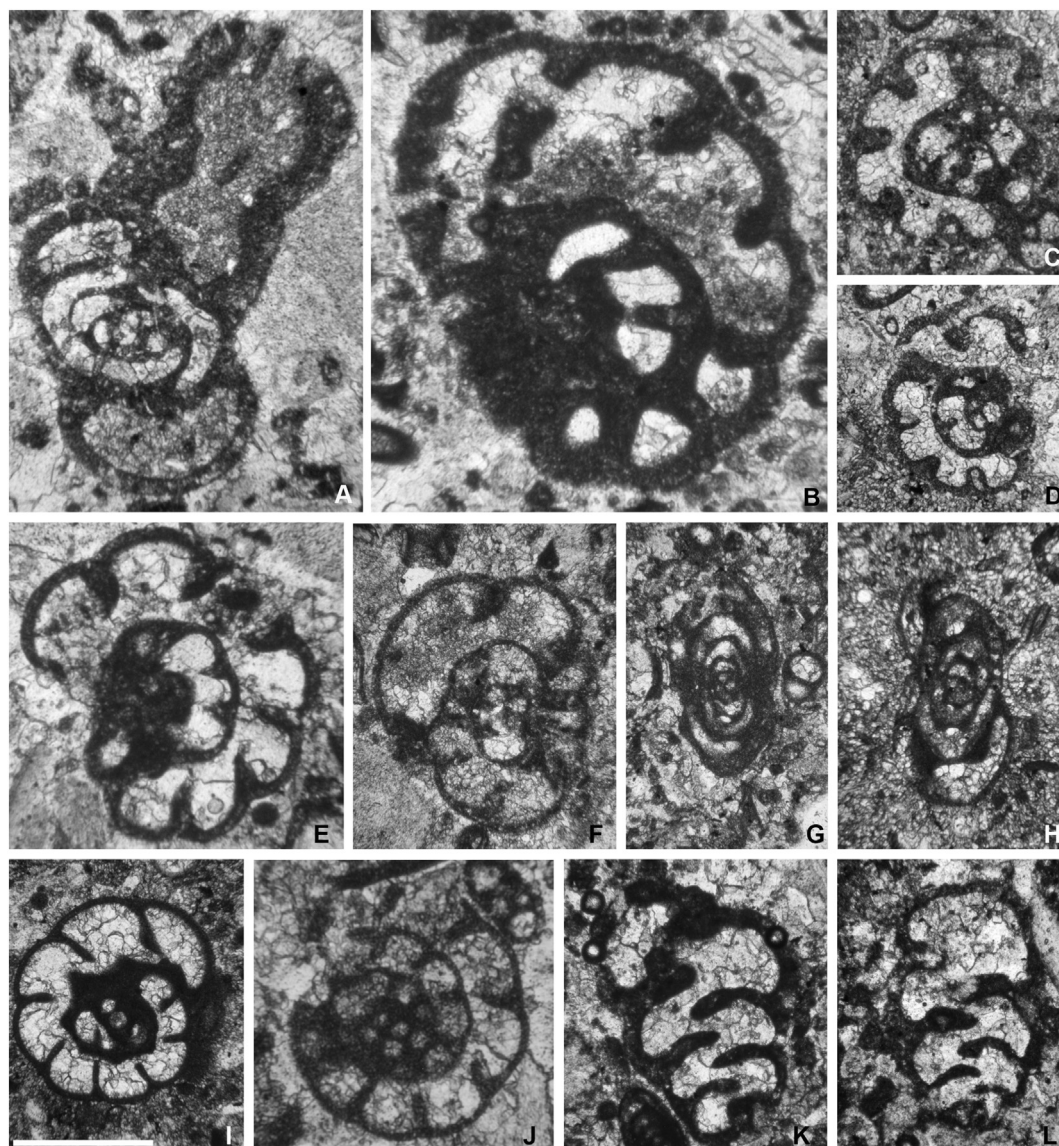


Fig. 15. Selected foraminifers from the Dalton Formation (scale bar 0.5 mm). A, *Lituotubella glomospiroides* Rauser-Chernousova, 1948a—sample BP3. B, *Cribranopsis* sp. 1—sample BP4. C, *Latiendothyranopsis solida* (Conil and Lys, 1964)—sample CG25. D, *Latiendothyranopsis* sp. 1—sample CG18. E, *Plectogyranopsis settlensis* (Conil and Longerstaey in Conil et al., 1980)—sample BP15x. F, *Plectogyranopsis moraviae* (Conil and Longerstaey in Conil et al., 1980)—sample BP19. G, *Eoparastaffella iniqua* Postojalko in Postojalko and Garan, 1972—sample BP9. H, *Eoparastaffella restricta* Postojalko in Postojalko and Garan, 1972—sample CG2. I, *Omphalotis* aff. *minima* (Rauser-Chernousova and Reitlinger in Rauser-Chernousova et al., 1936 sensu Cózár et al. (2022)—sample CG13. J, *Endothyranopsis* aff. *compressa* Rauser-Chernousova and Reitlinger in Rauser-Chernousova et al., 1936 sensu Cózár et al. (2022)—sample BP19. K, *Consobrinellopsis consobrina* (Lipina, 1948)—sample BP25. L, *Consobrinellopsis lipinae* (Conil and Lys, 1964)—sample BP25. See Supplementary information for precise sample location and taxa details.

facies than in the shallower-water facies. Hence, the Coastguard Quarry section shows the occurrence of all taxa, whereas in the Blackstone Point section, some of them occur slightly later than the uppermost Red Hill Limestone. The Cf4 δ subzone can be correlated with the MFZ11 γ of Cózár et al. (2020a), whereas it has no direct correlation with the zones defined by Poty et al. (2006). Conil et al. (1991) informally subdivided the Cf4 δ subzone into three intervals, with the lower and middle intervals characterised by the first occurrence of *Latiendothyranopsis solida*–*Endospiroplectammina syzranica*, and *Cribranopsis*–*Consobrinellopsis*–*Nodosarchaediscus*, respectively. *E. syzranica* has only been recorded in the Grubbins Wood 2 sections, whereas *Cribranopsis*, *L. solida* and *Nodosarchaediscus* have been recorded together in the basal metre of the Blackstone Point section and thus, they are not considered here as suitable markers for a subdivision of the Cf4 δ subzone. Overall, the assemblages remain rather similar throughout the Blackstone Member with the first significant changes recorded around the base of the Raven's Member.

In the mid-Blackstone Member and from lower levels in the Red Hill Limestone Formation at Low Frith (but most commonly from the Raven's Member), the precursor taxon *Endothyranopsis* aff. *compressa* (Rauser-Chernousova and Reitlinger in Rauser-Chernousova et al., 1936) sensu Cózár et al. (2022) (Fig. 15J), coincides with more evolved/occluded species of *Nodosarchaediscus* (Fig. 16H–J). However, in other sections, *E. aff. compressa* first occurs in older levels than these moderately occluded *Nodosarchaediscus* (e.g., Coastguard Quarry, Grubbins Wood 2 and Low Frith sections). The evolution in the degree of occlusion within *Nodosarchaediscus* can probably be considered as an auxiliary feature for subdivision of the Cf4 δ subzone. However, the validity of the genus has been questioned, owing to uncertainties of the type species (e.g., Brenckle and Grelecky, 1993), but the genus is widely used in the literature, even in recent classifications (e.g., Vachard, 2016). The first *Nodosarchaediscus* in the lower Cf4 δ subzone are rather questionable forms, with 1 or 2 whorls with nodes, and in some cases the nodes might be misidentifications of cement. From the

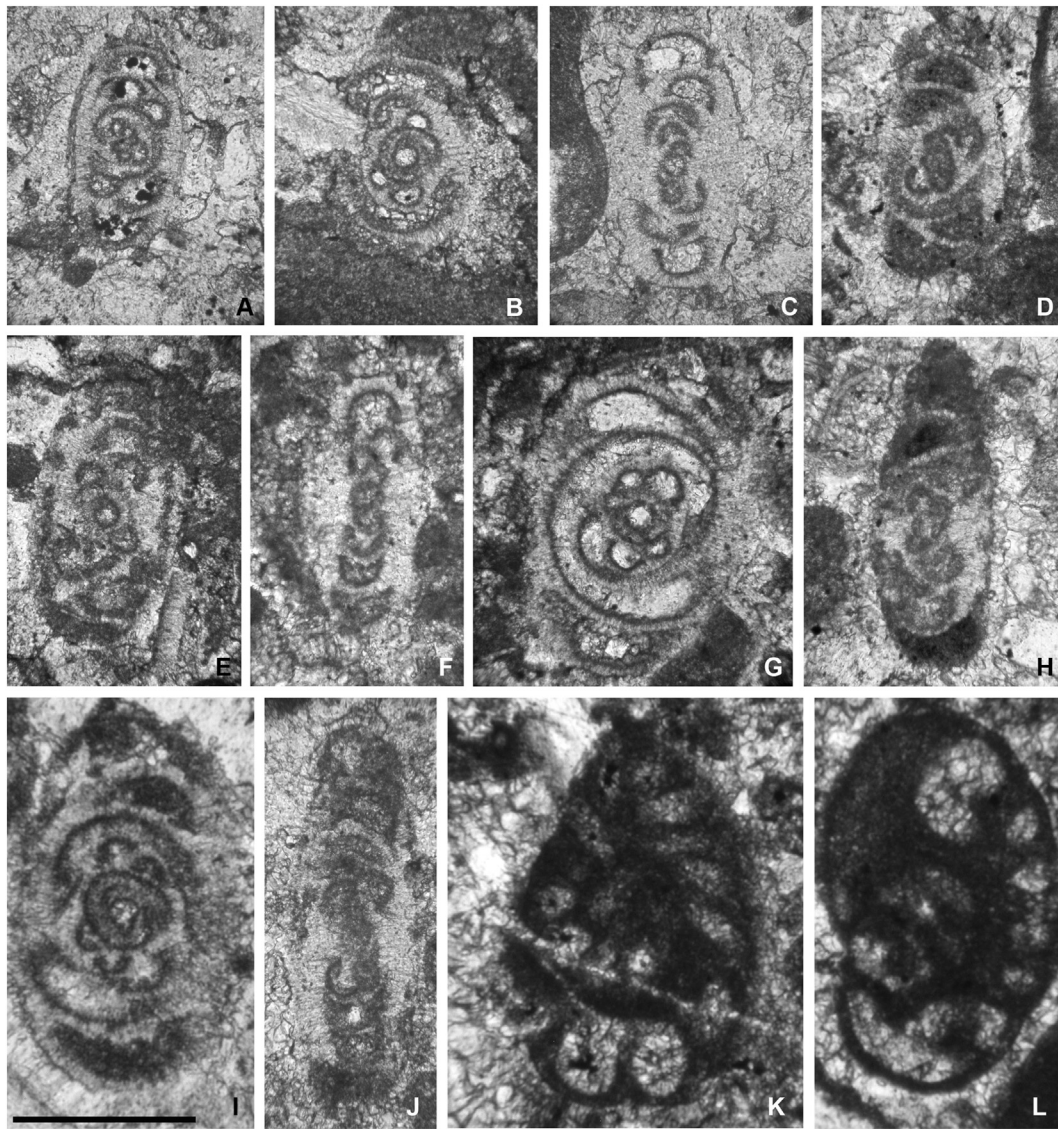


Fig. 16. Selected foraminifers from the Dalton Formation (scale bar 0.2 mm). A, *Archaeodiscus* sp. (transitional to the *convexus* stage)—sample BP8. B, *Archaeodiscus teres* Conil and Lys, 1964 (transitional to the *convexus* stage)—sample BP20. C, *Nodosarchaediscus?* sp.—sample BP11. D, *Nodosarchaediscus? cornua* (Conil and Lys, 1964)—sample BP12. E, *Nodosarchaediscus? viae* Vachard, 1977—sample BP14. F, *Nodosarchaediscus tchaboksarensis* (Bozorgnia, 1973)—sample BP18. G, *Archaeodiscus* aff. *convexus* Grozdilova and Lebedeva, in Dain and Grozdilova, 1953 (transitional to the *convexus* stage)—sample BP20. H, *Nodosarchaediscus conili* (Bozorgnia, 1973)—sample BP25. I, *Nodosarchaediscus hirta* (Conil and Lys, 1964)—sample BP29. J, *Nodosarchaediscus pirleti* (Bozorgnia, 1973)—sample BP27. K, Transitional form between *Eoparastaffella* and *Pojarkovella*—sample CG28. L, Transitional form between *Eoparastaffella* and *Pojarkovella*—sample BP30. See Supplementary information for precise sample locations.

Raven's Member more typical *Nodosarchaediscus* with nodes in several whorls occur such as; *N. exiguus* (Bozorgnia, 1973), *N. demaneti* (Conil and Lys, 1964), *N. hirta* (Conil and Lys, 1964) and *N. tchaboksarensis* (Bozorgnia, 1973). In both cases the presence of *Endothyranopsis* aff. *compressa* and *Nodosarchaediscus* s.s. coincides with the development of the purer limestones of the Raven's Member and thus there is a possibility that their presence could be facies controlled.

A relative facies control on the distribution of *Nodosarchaediscus* is apparent, as they are rare to absent in subtidal settings of the Raven's Member (Barker Scar and Coastguard Quarry sections), common in predominantly fluctuating intertidal–subtidal settings (such as in Grubbins Wood 1 section), and much more common in shallower-water facies (e.g., Blackstone Point section). This expresses a marked trend from deep- to shallow-water, but the occurrence of forms of *Nodosarchaediscus* could still be a useful guide. Moreover, *Eoendothyranopsis* aff. *donica* Brazhnikova and Rostovtseva in Brazhnikova et al. (1967) also occurs at White Scar Quarry, which is a marker of the Cf4δ subzone for Conil et al.

(1980), although owing to its scarcity it is not considered here as a reliable guide.

In higher levels of the Raven's Member, the foraminiferal assemblages are rather like those of the upper part of the Blackstone Member, although this part of the Raven's Member is characterised by the first occurrence of *Consobrinellopsis* (Fig. 15K–L) and an ancestral form of *Pojarkovella* (possibly transitional forms from evolved *Eoparastaffella*) (Fig. 16K–L). This part of the Cf4δ subzone seems to continue with the evolutionary trend in the degree of occlusion of the nodes of *Nodosarchaediscus*, and the strongly occluded forms that first occur are *N. pirleti* (Bozorgnia, 1973), *N. saleei* (Conil and Lys, 1964), *N. tchalussensis* (Bozorgnia, 1973) and *N. conili* (Bozorgnia, 1973). As in the older levels, these taxa seem to be more common in shallower water facies.

Hence, an informal subdivision of the Cf4δ subzone is proposed with divisions into 'lower', 'middle' and 'upper' (Fig. 13), although the precise characterisation of these assemblages as formal biostratigraphic subzones needs further investigation. Nevertheless, the

three subdivisions of Cf4 δ seem to mimic the correlation of the base of the Raven's Member and mid Raven's Member siliciclastic unit (Fig. 13), and thus are interpreted to be useful as a biostratigraphic tool for regional correlation in South Cumbria—although other factors such as facies control need further investigation for wider correlation.

The upper part of the Raven's Member in the Barker Scar section has been revised in detail by C  zar et al. (2022). The base of bed C at Barker Scar contains *Archaediscus* at *concaus* stage *sensu* Pirlet and Conil, 1977 (e.g., A. moelleri Rauser-Chernousova, 1948b, A. convexus Grozdilova and Lebedeva, in Dain and Grozdilova, 1953, A. pauxillus Shlykova, 1951 and oblique sections identified as spp.) and an ancestral form of *Koskinotextularia* (K. aff. *cribriiformis sensu* C  zar et al., 2022). These allow recognition of the Cf5 α subzone (C  zar et al., 2020a), although some other markers are not present (such as the primitive *Pojarkovella* species). Recorded in the upper part of bed C at Barker Scar are *P. honesta* Simonova in Simonova and Zub (1975), *P. occidentalis* Vachard and C  zar in Vachard et al. (2016), *P. ketmenica* Simonova and Zub (1975) and *P. pura* Simonova in Simonova and Zub (1975), and also the first occurrence of *P. nibelis* (Durkina, 1959)—allowing assignment to the Cf5 β subzone. Other typical markers of the Cf5 β subzone are recorded in much younger beds in the Park Limestone Formation, such as *Endothyranopsis compressa* (Rauser-Chernousova and Reitlinger in Rauser-Chernousova et al., 1936), *Koskinotextularia bradyi* (M  ller, 1879) and *K. cribriiformis* Eickhoff, 1968 (top of bed J), *Holkeria avonensis* (Conil and Longersstaey in Conil et al., 1980), *H. daggeri* Strank, 1982, *H. topleyensis* Strank, 1982 and *Koskinotextularia obliqua* (Conil and Lys, 1964) (from the base of bed K; Fig. 9). However, as discussed by C  zar et al. (2022) the lower part of the Barker Scar section is strongly affected by dolomitisation, and although the main markers are present in the section, they occur sparsely and their real stratigraphic first occurrences should be compared with other less dolomitised successions. The same interval is intersected in the Grubbins Wood-1 and White Scar Quarry sections (Fig. 9), of which the former shows very little dolomitisation, whilst the latter section has some dolomite patches and some beds of dolostone (Figs. 3, 9).

The Grubbins Wood 1 section contains most of the Raven's Member, although the transition into the Park Limestone Formation is not intersected within the section, but the basal Park Limestone is seen a short distance to the north in an escarpment (SI Fig. S2). At Grubbins Wood 1, foraminiferal assemblages similar to those of the Barker Scar section and assigned to the Cf5 α subzone are recorded at ca. 16.6 m from the base, whereas foraminiferal assemblages assigned to the Cf5 β subzone are recorded at ca. 21 m from the base (Fig. 9).

The White Scar Quarry section contains assemblages not quite as rich as those of Grubbins Wood-1, but is less-dolomitised than the Barker Scar section, and so contains a more continuous foraminiferal record with more diversity. At 19.4 m from the base, the Cf5 α subzone is recorded, and from 22 m the Cf5 β subzone occurs (Figs. 8, 9).

7. Discussion

7.1. Environmental interpretation of the facies distributions

The sections examined exhibit pronounced lateral facies changes over quite short distances, such as along the Arnside shore (Fig. 7). Hence, the ramp-model defined for South Cumbria by Adams et al. (1990, fig. 6) during the mid–late Arundian, with a slope directed southwards does not fully explain the facies variations observed. Mid to outer shelf facies, below fair-weather wave-base (FWWB) and either above or below the storm wave-base (SWB) are commonly recorded for the Blackstone Member in the Coastguard Quarry, Heversham and the preserved parts of the Barker Scar and Low Frith sections (subtidal in Fig. 13). However, the age-equivalent levels of the Blackstone Member in the other sections are rather different, with much shallower-water environments (intertidal and subtidal–intertidal). In these latter

sections, facies are predominantly intertidal grainstones (facies F9, F10), with a well-washed matrix (having only cements) or mixed intertidal/subtidal facies (F8), with exceptionally some levels attributed to purely subtidal conditions (facies F2, F3), such as at the Blackstone and Grubbins Wood 2 sections (Figs. 7, 9, 13).

A significant feature in the Blackstone Member in most sections are the common tempestite levels, or textures indicating reworking by storms (facies F4–F6; Figs. 7, 12). These storm-related facies suggest a middle shelf setting above SWB but below the FWFB, which contrasts markedly with the deeper-water settings at Barker Scar, Low Frith, Heversham and Coastguard Quarry sections in the Blackstone Member (Figs. 7, 9, 13). The general trend observed during sedimentation of the Blackstone Member shows deeper-water facies for the eastern part of the Arnside coast (Coastguard Quarry), Yewbarrow–Farleton and Leven Estuary areas, whereas the western parts of the Arnside coast indicate shallower conditions. This disposition suggests deeper water settings northwards, eastwards and westwards from the Blackstone–Grubbins Wood area. Thus, there seems not to be a single gradient of bathymetry southwards as proposed by Adams et al. (1990).

For the earliest part of the 'lower' Cf4 δ zone, typical grainstones assigned to the Red Hill Limestone Formation at Low Frith and Arnside shore sections, suggest shallower water conditions throughout, but with substantial thickness differences (Fig. 13). An alternative scenario for this earliest Cf4 δ interval may be that the siliciclastic transgression (i.e., base of the Blackstone Member) proceeded from east to west, such that shallower water conditions (i.e., topmost part of the Red Hill Formation) persisted in the Leven Estuary area for longer. However, this scenario is the opposite depth model to the overlying parts of the Blackstone Member.

During the lower part of the Raven's Member (approximately 'middle' Cf4 δ interval and beds A and B in the Barker Scar section), the same general trend is observed as in the Blackstone Member. Barker Scar and the preserved part in the Coastguard Quarry sections show deeper-water facies, whereas at the Grubbins Wood 1, Blackstone Point and White Scar Quarry sections, shallower-water facies are detected (Fig. 13). The distance between Barker Scar and the White Scar Quarry sections is approximately 14 km (Figs. 2, 13), which could justify this environmental difference, with the shelf becoming deeper to the west beginning from the western part of the Arnside Shore. This deepening could also be reflected in the dominance of wackestones (90% of succession; Nicholas, 1968) in the Dalton Formation further west in the Furness Peninsula. However, the strong dolomitisation at Barker Scar makes the preservation of facies poor (in some levels destroyed completely), whereas in others, dolomite is present in patches or samples are free or nearly-free of dolomitisation. This could have induced some erroneous identifications of clasts and matrix. In contrast, the lower Raven's Member in the Low Frith shore section, some 1.3 km north of Barker Scar, displays intertidal–subtidal microfacies indicating northwards shallowing.

Like Adams et al. (1990), we consider that the dolomitisation is a late diagenetic feature, in contrast to Ramsbottom's (1973) who suggested that dolomitisation was contemporaneous and associated with shallowing. Dolomitisation is more important in sections with deeper-water facies in this part of the shelf, which contradicts Ramsbottom's view. Dolomitisation is also more widespread in the Furness Peninsula, where it is a precursor (and largely spatially associated) with haematite mineralisation (Dunham and Rose, 1941; Nicholas, 1968, fig. 29), which could relate to the deeper water setting in the Furness Peninsula.

Thus, the variations between the three studied blocks during the Arundian cannot be explained with a single gradient of bathymetry and the sedimentation patterns seem to be delimitating swells and basins. Thickness variations over short distances, such as the Blackstone Member at Coastguard Quarry, which is nearly double the thickness of the other nearby other Arnside shore sections (Fig. 7), suggests that synsedimentary faulting was the source of these differences. This may also account for the shallowing in the Low Frith Shore section compared

to the same interval at Barker Scar (Fig. 13). In addition, thicknesses between the Raven's Member mid siliciclastic unit and the base of the Raven's Member are ca. 5.5 m at Barker Scar and 8.5 m at Blackstone Point (Figs. 7, 9), again suggesting differing accommodation space. The most likely source of the E–W changes are the NW–SE basement faults, which also currently segment the outcrops in this region (Fig. 2). Horbury (1987) also identified significant facies changes segmented by N–S boundaries in the lower park of the Asbian Urswick Limestone Formation.

The Dalton Formation corresponding to the Cf5 zone shows a change compared to the underlying beds, because intertidal conditions are predominant in all sections, and most samples are represented by grainstones facies F9–F10 (Figs. 9, 13). Tempestites are seldom recognised in the lower part of the Cf5 subzone or in the upper part of the studied sections (although they are common from overlying beds M to X in the Park Limestone at Barker Scar; Cózar et al., 2022). A predominant inner shelf is assigned to the Cf5 interval in the Dalton Formation. However, tectonic blocks were likely still active, allowing differential subsidence rates—the Cf5 interval below the topmost siliciclastics of the Raven's Member is ca. 16.5 m at Grubbins Wood, whereas at White Scar it is ca. 7.8, and in the Leven Estuary area is ca. 5.8 m (Fig. 13).

7.2. Significance of siliciclastics in the formations

The detrital zircon U–Pb age data indicates that a central Lake District 'high' was not a significant source of siliciclastics, since the Leinster–Lakesman terrane exhibits a major Ediacaran (540–640 Ma) zircon age peak and significant age contributions at 2–2.5 Ga (Waldron et al., 2019), something not seen in the Dalton Formation data (Fig. 11). Based on facies relationships Adams et al. (1990) also proposed no significant landmass in present-day central Cumbria for the late Arundian. However, on the Furness Peninsula and in NE Cumbria, Tournaisian–Chadian clastics which underlie the Viséan limestones units have clasts which can be matched to Lake District early Paleozoic units (Nicholas, 1968; Rose and Dunham, 1977; Kimber, 1987). This suggests either this Lake District source ceased to exist sometime in the late Chadian–early Arundian, or this clastic source was entirely focussed away from S. Cumbria. Adams et al. (1990) favoured the former possibility based on arguments of probable coastal onlap and typical rift basin evolution. Further provenance work in SW, W or NE Cumbria may shed light on the demise of the Lake District clastic source in the Mississippian.

The partial age equivalence of the 'Gastropod Beds' to the fluvially-derived sandstone units of NE Cumbria has been well-known since the work of Garwood (1913). Johnson et al. (2001) also highlighted the importance of terrigenous inputs into the Dalton Formation, an interval now included in the top–most part of the Raven's Member. Quartz grains are also commonly present in all the studied sections (Section 5.12), but some parts show higher concentrations of quartz grains (facies F12), and thus a stronger siliciclastic input. The most consistently sandy interval is the upper–most part of the Raven's Member and into the lowest Park Limestone Formation (Fig. 13). Like others, Adams et al. (1990) compared these sandy levels with the Ashfell Sandstone of the Ravenstonedale area, which has been attributed to a clastic coastal system (Stanway et al., 2015) coeval with the fluvial Fell Sandstone in the Northumberland Trough. According to Wakefield et al. (2016) and Kearsy et al. (2019), these clastic systems were derived via major fluvial systems in the central and northern North Sea during the Arundian. Certainly, compared to the Barker Scar section, the occurrence of more sandy levels at White Scar Quarry is suggestive of a more northeastern source for these clastics, like the Arundian palaeogeography suggested by Wakefield et al. (2016). The Ashfell Sandstone was assigned to the Cf4 δ –Cf5 α subzones in Waters et al. (2021), and sandstones are also recorded in the Frizington Formation of northwest Cumbria (Barclay et al., 1994; Akhurst et al., 1997), which has been attributed to the lower part of the Cf5 β subzone by Waters et al. (2021). The alternative Southern Uplands source of this

detritus may have been via the siliciclastic rich Viséan successions of the northern Solway Basin (Deegan, 1973; Maguire et al., 1996). The sand-prone fluvial systems in parts of the northern Solway successions do show westwards transport (Maguire et al., 1996; Leeder, 1974), implicating axial flow as suggested by Wakefield et al. (2016), but northerly derived clastics from unroofing of the Devonian granites in the southern Uplands were also a major local source of clastics in the Viséan (Craig, 1957; Craig and Nairn, 1956; Deegan, 1973). Marine dispersal of this material via storms and wave transfer southwards of both the sandy and fine-grained siliciclastics, may have provided a more direct northerly route via NW Cumbria, albeit rather more distant than the Ashfell Sandstone route. The zircon and apatite U–Pb ages also suggest derivation from the north, but with a more distal Lewisian-like source (and a lesser contribution), mixing with detritus from the Southern Upland terrane. The similarity in age spectra between the mid and late Raven's Member clastic detritus suggests that this source was similar throughout the Dalton Formation.

The combined facies data from the Dalton and lower part of the Park Limestone formation indicates a progressive regional shallowing into the Cf5 β 1 subzone (Fig. 13). Riley (1993) proposed a non-sequence in the Barker Scar section at the base of bed I (Figs. 9, 10D) due to the absence of Garwood's *Cyrtina carbonaria* Beds, and the lack of transitional coral faunas seen in North Wales and Northern Ireland. A sandy palaeosol in the Canal Foot quarry at about this level (Johnson et al., 2001) was also implicated as an expression of this hiatus. However, the regional development of a significant palaeosol in the uppermost Raven's Member is not clear, since whilst we also detect a weakly developed gleyed-palaeosol at White Scar Quarry, other sedimentological evidence of significant erosion at this level is absent. The absence of the *C. carbonaria* Beds could be misleading, since Garwood (1913) made no distinction from the overlying '*Nematophyllum minus*' Subzone in this region of S. Cumbria, and this brachiopod may be facies dependent. Evidence of erosional loss via down-cutting units is most evident at Barker Scar, where the base of beds at 6.1 m, 10.5 m and 24.6 m could represent a non-sequence (Fig. 9, SI Fig. S8). However, the consistency of the foraminiferal data as demonstrated by the continuous foraminiferal record at Barker Scar (Cózar et al., 2022) and the other sections (Fig. 13) argues against a significant hiatus near the top of the Raven's Member. Rather, the elevated siliciclastic input at this level may simply reflect a maximum of distal inputs into a shallowing shelf. Sandy limestones and dolostones also occur at other levels in the Barker Scar section in beds E, F, H, and locally in bed I (Cózar et al., 2022). Sandy limestones in similar stratigraphic positions also occur at White Scar Quarry (Fig. 13). All these levels likely represent distal dispersion events either from the front of the coastal system of the Ashfell Sandstone situated some 35 km to the NE, or from the northern parts of the Solway Basin some 90 km to the North.

8. Conclusions

We have revised the lithostratigraphy and biostratigraphy of the Lower to Middle Viséan (mid Arundian–early Holkerian) strata of South Cumbria comprising the Dalton Formation, lowest parts of the Park Limestone Formation, and parts of the Red Hill Limestone Formation. Conclusions are:

1. The Dalton Formation has been subdivided into two members an older Blackstone Member and a younger Raven's Member which can be traced throughout the region. Type sections are proposed at Blackstone Point and White Scar Quarry, respectively.
2. Bentonitic shales are recorded for the first time in South Cumbria and are developed in the mid and top parts of the Raven's Member and could potentially form useful regional synchronous markers.
3. U–Pb zircon and apatite ages from the bentonitic layers in the Raven's Member are almost all detrital, with zircon U–Pb age spectra indicating provenance from the Southern Uplands terrane to the

north or NE, and apatite U–Pb age data indicating lesser first cycle sourcing, from the more distal Lewisian Complex of NW Scotland or eastern Greenland sources. The Lakesman Terrane did not provide a significant source of this detritus.

- Limestones of the Dalton Formation contain rich foraminiferal assemblages ranging in age from the late Arundian to early Holkerian. The upper part of the Raven's Member records the first appearance of taxa assigned to the Cf5 α and Cf5 β subzones of Holkerian age. The base of the late Arundian Cf4 δ subzone is within the topmost Red Hill Limestone Formation in the Arnside–Silverdale region, whereas in the Leven Estuary area it occurs lower in this formation. This either indicates some diachroneity of the base of the Dalton Formation, or substantially different accumulation rates near the base of the Cf4 δ subzone.
- Petrographic analysis identified 13 microfacies with a dominance of argillaceous wackestone and packstone in the Blackstone Member and peloidal bioclastic intraclastic grainstones in the Raven's Member and lower Park Limestone Formation. These facies developed on the inner to outer part of a dominantly southward dipping shelf. The shelf was segmented by NW–SE basement faults producing significant synsedimentary segmentation of facies into separate blocks and a westward deepening of facies in the lower and mid parts of the Dalton Formation. Although the lateral facies changes affected all the units, there is a predominance of inner shelf facies in the Red Hill Limestone Formation, outer to middle shelf settings in the Blackstone Member, middle shelf conditions for the lower and middle Raven's Member, and middle to mostly inner shelf for the upper Raven's Member and lower part of the Park Limestone Formation.
- Fine siliciclastic material (30–150 μm in size) occurs in the limestones of the Raven's Member and lowest Park Limestone Formation and likely represents dispersal from the siliciclastic dominated late Arundian–early Holkerian coastal systems to the northeast in Cumbria or the northern Solway Basin. The continuity of foraminiferal assemblages and lack of coeval sedimentological evidence of significant non-sequence suggests the more siliciclastic-rich levels are not by themselves evidence of hiatus.

Declaration of competing interest

The authors declare that they have no known competing financial interest or personal relationships that could have appeared to influence the work reported in this paper.

Acknowledgements

We are grateful to the comments by E. Kulagina and an anonymous reviewer. MWH was in part funded by NERC (grant NE/P00170X/1). PC is grateful to the financial support by the project CGL2016-78738 of the Spanish Ministry of Science and Innovation. DC is supported in part by a research grant from Science Foundation Ireland (SFI) under Grant Number 13/RC/2092_P2 (iCRAG, the SFI Research Centre in Applied Geosciences). Vassil Karloukovski, Tereza Kamenikova, David Mindham, Courtney Sprain and Shihu Li helped collect some of the samples. The log and sampling for Grubbins 2a and 2b sections, was co-measured by Cathy Hollis. Natural England, Cumbria Wildlife Trust, Holker Hall Estate, the Arnside Silverdale AONB, and the Landowners of Crosthwaite and Lyth, allowed access, permission and permits to collect samples from these sections.

Appendix A. Supplementary data

Supplementary data associated with this article can be found in the online version at <https://doi.org/10.1016/j.pgeola.2022.04.005>. These

data include the Google map of the most important areas described in this article.

References

- Adams, A.E., 1984. Development of algal-foraminiferal-coral reefs in the lower carboniferous of furness, Northwest England. *Lethaia* 17, 233–249.
- Adams, A.E., Horbury, A.D., Abdel Aziz, A.A., 1990. Controls on dinantian sedimentation in South Cumbria and surrounding areas of Northwest England. *Proceedings of the Geologists' Association* 101, 19–30.
- Akhurst, M.C., Chadwick, R.A., Holliday, D.W., McCormac, M., McMillan, A.A., Millward, D., Young, B., 1997. *Geology of the west Cumbria district. Memoir of the British Geological Survey, sheets 28, 37 and 47 (England and Wales)*. HMSO BGS, Keyworth, Nottingham (138 pp.).
- Baccelle, L., Bosellini, A., 1965. Diagrammi per la stima visiva della composizione percentuale nelle rocce sedimentarie. *Annali della Università di Ferrara, Sezione IX, Science Geologiche e Paleontologiche* 1 (1), 59–62.
- Balderstone, M., Dewey, M., 2003. The Dinantian Limestones of the Far Arnside and Silverdale Shoreline. *Proceedings of the Westmorland Geological Society* 31, 6–22.
- Barclay, W.J., Riley, N.J., Strong, G.E., 1994. The dinantian rocks of the sellafield area, West Cumbria. *Proceedings of the Yorkshire Geological Society* 50, 37–49.
- Bozorgnia, F., 1973. Paleozoic foraminiferal biostratigraphy of central and east Alborz MountainsIran, National Iranian Oil Company, Geological Laboratories, Publication, 4, pp. 1–185.
- Brazhnikova, N.E., Vakartchuk, G.I., Vdovenko, M.V., Vinnichenko, L.V., Karpova, M.A., Kolomiets, L.L., Potievskaya, P.K., Rostovtseva, L.P., Shevchenko, G.D., 1967. Microfaunal marker horizons in Carboniferous and Permian deposits of the Dniéper–Donetsk Basin. *Izdatel'stvo "Naukova Dumka", Kiev (in Russian)*.
- Brenckle, P.L., Grelecky, J.C., 1993. Type archaeiscacean foraminifers (Carboniferous) from the former Soviet Union and Great Britain, with a description of computer modelling of archaeiscacean coilingCushman, Foundation for Foraminiferal Research, Special Publication, 30, pp. 1–58.
- Chew, D., O'Sullivan, G., Caracciolo, L., Mark, C., Tyrrell, S., 2020. Sourcing the sand: accessory mineral fertility, analytical and other biases in detrital U–pb provenance analysis. *Earth-Science Reviews* 202. <https://doi.org/10.1016/j.earscirev.2020.103093>.
- Conil, R., Lys, M., 1964. Matériaux pour l'étude micropaléontologique du Dinantien de la Belgique et de la France (Avesnois). Pt. 1, Algues et foraminifères; Pt. 2, Foraminifères (suite). *Mémoires de l'Institut de Géologie de l'Université de Louvain*, 23, pp. 1–372.
- Conil, R., Naum, C., 1976. Les foraminifères du Viséen moyen V2a aux environs de Dinant. *Annales de la Société Géologique de Belgique* 99, 109–142.
- Conil, R., Longerstaey, P.J., Ramsbottom, W.H.C., 1980. Matériaux pour l'étude micropaléontologique du Dinantien de Grande-Bretagne, Mémoires de l'Institut de Géologie de l'Université de Louvain, 30, pp. 1–187 (printed 1979).
- Conil, R., Groessens, E., Laloux, M., Poty, E., Tourneur, F., 1991. Carboniferous guide foraminifera, corals and conodonts in the Franco-Belgian and Campine basins. Their potential for widespread correlation. *Courier Forschungsinstitut Senckenberg* 130, 15–30.
- Cossey, P.J., Adams, A.E., Purnell, M.A., Whiteley, M.J., Whyte, M.A., Wright, V.P., 2004. British lower carboniferous stratigraphy. *Geological conservation review series 29*. Joint Nature Conservation Committee, Peterborough, p. 636.
- Cózar, P., Somerville, I.D., 2020. Foraminifers in upper Viséan-lower Serpukhovian limestones from South Wales: regional correlation and implications for the British foraminiferal zonal schemes. *Proceedings of the Yorkshire Geological Society* 63, pygs2020-009. <https://doi.org/10.1144/pygs2020-009>.
- Cózar, P., Izart, A., Somerville, I.D., Aretz, M., Coronado, I., Vachard, D., 2019. Environmental controls on the development of mississippian microbial carbonate mounds and platform limestones in southern montagne noire (France). *Sedimentology* 66, 2392–2424.
- Cózar, P., Vachard, D., Somerville, I.D., Izart, A., Coronado, I., 2020a. Lower-middle Viséan boundary interval in the palaeotethys: refinements for the foraminiferal zonal schemes. *Geological Magazine* 157, 513–526.
- Cózar, P., Vachard, D., Izart, A., Said, I., Somerville, I., Rodríguez, S., Coronado, I., El Houicha, M., Ouarhache, D., 2020b. Lower-middle Viséan transgressive carbonates in Morocco: palaeobiogeographic insights. *Journal of African Earth Sciences* 168, 103850. <https://doi.org/10.1016/j.jafrearsci.2020.103850>.
- Cózar, P., Somerville, I.D., Hounslow, M.W., 2022. Foraminifers in the holkerian stratotype, regional substage in Britain: key taxa for the Viséan subdivision. *Newsletters in Stratigraphy* 55, 159–172. <https://doi.org/10.1127/nos/2021/0674>.
- Cózar et al., n.d. P. Cózar I.D. Somerville M.W. Hounslow T. Kamenikova, in press. Proposal of a late Asbian (Mississippian) stratotype for England: Trowbarrow Quarry, S. Cumbria, UK. *Papers in Palaeontology*.
- Craig, G.Y., 1957. VII.—The lower carboniferous outlier of Kirkbean, Kirkcudbrightshire. *Transactions of the Geological Society of Glasgow* 22, 113–132.
- Craig, G.Y., Nairn, A.E.M., 1956. The lower carboniferous outliers of the colvend and rerrick shores, Kirkcudbrightshire. *Geological Magazine* 93, 249–256.
- Dain, L.G., Grozdilova, L.P., 1953. Iskopaemye foraminifery SSSR: Turneiellidy i Arkhedistsidy (Tournayellidae). In: Dain, L.G., Grozdilova, L.P. (Eds.). *Fossil foraminifers of the USSR, Tournayellidae and Archaeiscidae*, *Proceedings of the Oil Research Geological Institut (VNIGRI)*, 74, pp. 1–115 (in Russian).
- Dean, M.T., Browne, M.A.E., Waters, C.N., Powell, J.H., 2011. A lithostratigraphical framework for the Carboniferous successions of Northern Great Britain (onshore). *British Geological Survey Research Report, RR/10/07*. HMSO, London (174 pp.).
- Deegan, C.E., 1973. Tectonic control of sedimentation at the margin of a carboniferous depositional basin in Kirkcudbrightshire. *Scottish Journal of Geology* 9, 1–28.

- Dunham, R.J., 1962. Classification of carbonate rocks according to depositional texture. In: Ham, W.E. (Ed.), *Classification of Carbonate Rocks*, American Association of Petroleum Geologists, Memoir, 1, pp. 108–121.
- Dunham, K.C., Rose, W.C.C., 1941. Geology of the iron-ore field of South Cumberland and furness, Wartime Pamphlet, Geological Survey of Great Britain, 16, pp. 1–26.
- Durkina, A.V., 1959. Foraminifery nizhnemennougolnykh otlozhenii Timano-Pechorskoi provintsi (Foraminifers from Early Carboniferous of Timan-Pechora province), *Mikrofauna SSSR* 10, Trudy Vsesoyuznogo Nauchno-Issledovatel'skogo Geologorazvedochnogo Instituta, 136, pp. 132–335 (in Russian).
- Eickhoff, G., 1968. Neue textularien (Foraminifera) aus dem Waldecker Unterkarbon. *Paläontologisches Zeitschrift* 42, 162–178.
- Embry, A.F., Klovan, J.E., 1971. A late devonian reef tract on northeastern Banks Island, NWT. *Bulletin of Canadian Petroleum Geology* 19, 730–781.
- Fewtrell, M.D., Ramsbottom, W.H.C., Strank, A.R.E., 1981. Carboniferous. In: Jenkins, D.G., Murray, J.W. (Eds.), *Stratigraphical atlas of fossil Foraminifera*, British Micropalaeontological Society Series. Ellis Horwood, Chichester, pp. 13–69.
- Flügel, E., 2004. *Microfacies of carbonate rocks*. Analysis, interpretation and application. Springer Verlag, Berlin, Heidelberg, NewYork (976 pp.).
- Garwood, E.J., 1913. The lower carboniferous succession in the north-west of England. *Quarterly Journal of the Geological Society of London* 68, 449–572.
- Garwood, E.J., 1916. The faunal succession in the lower carboniferous rocks of Westmorland and North Lancashire. *Proceeding of the Geologists' Association* 27, 1–43.
- George, T.N., Johnson, G.A.L., Mitchell, M., Prentice, J.E., Ramsbottom, W.H.C., Sevastopulo, G.D., Wilson, R.B., 1976. A correlation of Dinantian rocks in the British Isles. *Geological Society, London, Special Report*, 7 (87 pp.).
- Horbury, A.D., 1987. *Sedimentology of the urswick limestone in South Cumbria and North Lancashire*. PhD thesis University of Manchester, UK (unpublished).
- Johnson, E.W., Soper, N.J., Burgess, I.C., 2001. *Geology of the country around ulverston*. Memoir of the British Geological Survey, sheet 48 (England and Wales). HMSO, London (129 pp.).
- Kalvoda, J., Bábek, O., Devuyt, F.X., Sevastopulo, G.D., 2011. Biostratigraphy, sequence stratigraphy and gamma-ray spectrometry of the tournaïsan-Viséan boundary interval in the Dublin Basin. *Bulletin of Geosciences* 86 (4), 683–706.
- Kearsey, T.I., Millward, D., Ellen, R., Whitbread, K., Monaghan, A.A., 2019. Revised stratigraphic framework of pre-westphalian carboniferous petroleum system elements from the outer Moray firth to the Silverpit Basin, North Sea, UK. *Geological Society, London, Special Publications* 471 (1), 91–113.
- Kimber, R.N., 1987. *The Carboniferous basement rocks of northern Britain*. Durham Univ (Unpubl. PhD thesis).
- Lancaster, P.J., Daly, J.S., Storey, C.D., Morton, A.C., 2017. Interrogating the provenance of large river systems: multi-proxy in situ analyses in the millstone grit, Yorkshire. *Journal of the Geological Society* 174, 75–87. <https://doi.org/10.1144/jgs2016-069>.
- Leeder, M.R., 1974. Lower border group (Tournaisian) fluvio-deltaic sedimentation and palaeogeography of the Northumberland Basin. *Proceedings of the Yorkshire Geological Society* 40, 129–180.
- Lipina, O.A., 1948. *Tekstulyariidy verkhnei chasti nizhnego Karbona Yuzhnogo Kryla Podmoskovnogo Basseina (Textulariids of the upper part of Early Carboniferous from southern margin of the Moscow Basin)*, Akademiya Nauk SSSR, Trudy Instituta Geologicheskikh Nauk 62 geologicheskaya seriya, 19, pp. 196–215 (in Russian).
- Maguire, K., Thompson, J., Gowland, S., 1996. Dinantian depositional environments along the northern margin of the Solway Basin, UK. In: Strogen, P., Somerville, I.D., Jones, G.L. (Eds.), *Recent Advances in Lower Carboniferous Geology*, Geological Society, London, Special Publications, 107, pp. 163–182.
- Malakhova, N.P., 1975. Foraminifery, vodorosli i stratigrafiya nizhnego vize vostochnogo sklona Yuzhnogo Urala (Foraminifers, algae and stratigraphy of the early Viséan of the western slope of southern Urals). In: Malakhova, N.P., Chuvashov, B.I. (Eds.), *Foraminifery i stratigrafiya rannego vize Urala (Foraminifers and stratigraphy from early Viséan of Urals)*, Akademiya Nauk SSSR, Uralskii Nauchnyi Tsentr, Trudy Instituta Geologii i Geokhimii, 112, pp. 71–109 (in Russian).
- McCoy, F., 1844. A synopsis of the characters of the carboniferous limestone fossils of Ireland. McCoy, Dublin (<sb:pages>207 pp.</sb:pages>).
- Mikhailov, A., 1939. K kharakteristike rodov nizhnemennougolnykh foraminifer territorii SSSR; nizhnemennougolnye otlozheniya severo-zapadnogo kryla podmoskovnogo basseina (On characteristic genera of early carboniferous foraminifers in territories of the USSR; the lower carboniferous deposits of the northwestern limb of Moscow basin). *Sbornik Leningradskogo Geologicheskogo Upravleniya* 3, 47–62 (in Russian).
- Millward, D., McCormac, M., Soper, N.J., Woodcock, N.H., Rickards, R.B., Butcher, A., Entwistle, D., Raines, M.G., 2010. *Geology of the Kendal district*, a brief explanation of the geological map sheet 39 Kendal, Sheet explanation of the British Geological Survey, 1:50000 sheet 39 Kendal. HMSO, Keyworth, p. 34.
- Möller, V.v., 1879. Die Foraminiferen des russischen Kohlenkalks, Mémoires de l'Académie Impériale des Sciences de St. Pétersbourg, 7th series, 27, pp. 1–131.
- Morton, A.C., Hallsworth, C.R., 1999. Processes controlling the composition of heavy mineral assemblages in sandstones. *Sedimentary Geology* 124, 3–29.
- Morton, A.C., Chisholm, J.L., Frei, D., 2021. Provenance of carboniferous sandstones in the central and southern parts of the Pennine Basin, UK: evidence from detrital zircon ages. *Proceedings of the Yorkshire Geological Society* 63, pygs2020-010. <https://doi.org/10.1144/pygs2020-010>.
- Nicholas, C., 1968. *The stratigraphy and sedimentary petrology of the lower carboniferous rocks south west of the Lake District*. Unpublished Ph.D. Thesis University of London.
- Pille, L., 2008. Foraminifères et algues calcaires du Mississippien supérieur (Viséan supérieur-Serpukhovien): rôles biostratigraphique, paléocécologique et paléogéographique aux échelles locale, régionale et mondiale. Thèse Université de Lille 1, 3 volumes (327 pp., 256 pp., 150 pp.) (unpublished).
- Pirlet, H., Conil, R., 1977. L'évolution des archaediscaïdes viséens. *Bulletin de la Société belge de Géologie* 82, 241–299.
- Pointon, M.A., Cliff, R.A., Chew, D.M., 2012. The provenance of Western Irish Namurian Basin sedimentary strata inferred using detrital zircon U-Pb LA-ICP-MS geochronology. *Geological Journal* 47, 77–98.
- Postojalko, M.V., Garan, I.M., 1972. Fauna of the pesterkovsky horizon of the early Viséan of the western slope of the middle urals. *Trudy Instituta Geologii i Geokhimii* 101, 3–18 (in Russian).
- Poty, E., Devuyt, F.-X., Hance, L., 2006. Upper devonian and mississippian foraminiferal and rugose coral zonation of Belgium and northern France: a tool for eurasian correlations. *Geological Magazine* 143, 829–857.
- Ramsbottom, W.H.C., 1973. Transgressions and regressions in the dinantian: a new synthesis of british dinantian stratigraphy. *Proceedings of the Yorkshire Geological Society* 39, 567–607.
- Ramsbottom, W.H.C., 1981. Field guide to the boundary stratotypes of the Carboniferous stages in Britain. *Biennial Meeting of the Subcommission of Carboniferous Stratigraphy*, Leeds (110 pp.).
- Rauscher-Chernousova, D.M., 1948. Rod Haplophragmella i blizkie k nemy formy (Genus Haplophragmella and related forms), Akademiya Nauk SSSR, Trudy Instituta Geologicheskikh Nauk, 62, geologicheskaya seriya, 19, pp. 159–165 (in Russian).
- Rauscher-Chernousova, D.M., 1948. Nekotorye novye vidy foraminifer iz nizhnemennougolnykh otlozhenii Podmoskovnogo basseina (Some new species of foraminifera of the Early Carboniferous deposits of the Moscow Basin), Akademiya Nauk SSSR, Trudy Instituta Geologicheskikh Nauk, 62, geologicheskaya seriya, 19, pp. 227–238 (in Russian).
- Rauscher-Chernousova, D.M., 1948c. Materialy k faune foraminifer kamenougolnykh otlozhenii Tsentralnogo Kazakhstana (Materials for foraminiferal fauna from the Carboniferous deposits from central Kazakhstan), Akademiya Nauk SSSR, Trudy Instituta Geologicheskikh Nauk 66, geologicheskaya seriya, 21, pp. 1–66 (in Russian).
- Rauscher-Chernousova, D.M., Belyaev, G.M., Reitlinger, E.A., 1936. Verkhnepaleozoiskie foraminifery Pechorskogo Krya (Late paleozoic foraminifera from the Pechora territory). *Trudy Polyarnoy Komissii* 28, 152–232 (in Russian).
- Riley, N.J., 1993. Dinantian (Lower Carboniferous) biostratigraphy and chronostratigraphy in the British Isles. *Journal of the Geological Society of London* 150, 427–446.
- Rose, W.C.C., Dunham, K.C., 1977. *Geology and hematite deposits of South Cumbria*, Economic memoir of the geological survey of Great Britain, sheets 58 and part of 48. HMSO, London, p. 170.
- Shlykova, T.I., 1951. Stratigraphy and microfauna of the lower carboniferous of the western wing of the Moscow region. *Proceedings of the Oil Research Geological Institut (VNIGRI)* 56, 109–178 (in Russian).
- Simonova, Y.A., Zub, B.B., 1975. Novye predstaviteli semeitsva Quasiendothyridae iz sredne-verkhnevizeiskikh otlozhenii severnogo Tian-Shanya i Malogo Karatau (New representatives of the family quasiendothyridae from the middle-late Viséan of north tian-shan and lesser Kara-Tau). *Trudy Kazakhskogo Politekhnikeskogo Instituta Geologiya* 1975 (9), 19–35 (in Russian).
- Stanway, P., Nudds, J., Broadhurst, F., 2015. The depositional environment of the ashfell sandstone formation (Arundian, Mississippian), ash fell edge, Cumbria, NW England. *Proceedings of the Yorkshire Geological Society* 60, 145–152.
- Strank, A.R.E., 1981. Foraminiferal biostratigraphy of the holkerian, asbian and brigantian stages of the british lower carboniferous. Ph.D. Thesis University of Manchester, Manchester (391 pp.) (unpublished).
- Strank, A.R.E., 1982. Holkeria gen. nov. A foraminifer characteristic of the Holkerian stage of the British Dinantian. *Proceedings of Yorkshire Geological Society* 44, 145–151.
- Thomas, P.R., 2009. *Geology of the area between Lindale and Witherslack*. Geology and landscapes northern Britain programme. British Geological Survey, Internal Report IR/06/079. HMSO, Keyworth (30 pp.).
- Tyrrill, S., Houghton, P.D.W., Daly, J.S., Kokfeft, T.F., Gagnevin, D., 2006. The use of the common Pb isotope composition of detrital K-feldspar grains as a provenance tool and its application to upper carboniferous paleodrainage, northern England. *Journal of Sedimentary Research* 76, 324–345.
- Vachard, D., 1977. Etude stratigraphique et micropaléontologique (algues et foraminifères) du Viséan de la montagne noire (Hérault, France). *Mémoires Institut Géologique Université Louvain* 29, 111–195.
- Vachard, D., 2016. Macroevolution and biostratigraphy of paleozoic foraminifer. In: Montanari, M. (Ed.), *Stratigraphy & Timescales*. Elsevier, Amsterdam, pp. 257–323.
- Vachard, D., Tahiri, A., 1991. Foraminifères, algues et pseudoalgues du Viséan de la région d'Oulmès (Maroc). *Géologie Méditerranéenne* 43, 21–41.
- Vachard, D., Cózar, P., Aretz, M., Izart, A., 2016. Late Viséan-early serpukhovian foraminifers in the montagne noire (France): biostratigraphic revision and correlation with the russian substages. *Geobios* 49, 469–498.
- Vaughan, A., 1905. *Palaeontological sequence in the carboniferous limestone of the Bristol area*. Quarterly Journal of the Geological Society, London 61, 181–307.
- Wakefield, O., Waters, C.N., Smith, N.J.P., 2016. Carboniferous stratigraphical correlation and interpretation in the Irish Sea. *British Geological Survey Commissioned Report*, CR/16/040 (82 pp.).
- Waldrón, J.W.F., Floyd, J.D., Simonetti, A., Heaman, L.M., 2008. Ancient laurentian detrital zircon in the closing lapetus Ocean, southern uplands terrane, Scotland. *Geology* 36, 527–530.
- Waldrón, J.W., Schofield, D.I., Pearson, G., Sarkar, C., Luo, Y.A.N., Dokken, R., 2019. Detrital zircon characterization of early cambrian sandstones from east avalonia and SE Ireland: implications for terrane affinities in the peri-gondwanan caledonides. *Geological Magazine* 156, 1217–1232.
- Waters, C.N., Waters, R.A., Barclay, W.J., Davies, J.R., 2009. A lithostratigraphical framework for the carboniferous successions of southern Great Britain (Onshore), British Geological Survey research report, RR/09/01. HMSO, London, p. 184.

Waters, C.N., Dean, M.T., Jones, N.S., Somerville, I.D., 2011. Chapter 12. Cumbria and the northern Pennines. In: Waters, C.N., Somerville, I.D., Jones, N.S., et al. (Eds.), *A revised correlation of Carboniferous rocks in the British Isles*. The Geological Society, London, Special Report, 26, pp. 82–88.

Waters, C.N., Burgess, I.C., Cózar, P., Holliday, D.W., Somerville, I.D., 2021. Reappraisal of arundian–asbian successions of the great scar limestone group across northern England. *Proceedings of the Yorkshire Geological Society* 63, pygs2021-02. <https://doi.org/10.1144/pygs2021-002>.